AFOSR 69-0189 TR

Methods of Magnetotelluric Analysis

By
William E. Sims and F. X. Bostick, Jr.
Department of Electrical Engineering

Technical Report No. 58
January 7, 1969

ELECTRICAL GEOPHYSICS RESEARCH LABORATORY

prepared under
Grant GA-1236
National Science Foundation
and
Contract N00014-67-A-0216-0004
Office of Naval Research
Washington, D.C.

ELECTRONICS RESEARCH CENTER
THE UNIVERSITY OF TEXAS AT AUSTIN
AUSTIN, TEXAS 78712

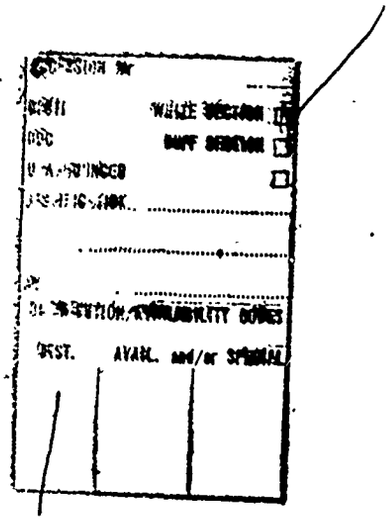

The Electronics Research Center at The University of Texas at Austin constitutes interdisciplinary laboratories in which graduate faculty members and graduate candidates from numerous academic disciplines conduct research.

Research conducted for this technical report was supported in part by the Department of Defense's JOINT SERVICES ELECTRONICS PROGRAM (U.S. Army, U.S. Navy, and U.S. Air Force) through the Research Grant AF-AFOSR-67-766E. This program is monitored by the Department of Defense's JSEP Technical Advisory Committee consisting of representatives from the U.S. Army Electronics Command, U.S. Army Research Office, Office of Naval Research and the U.S. Air Force Office of Scientific Research.

Additional support of specific projects by other Federal Agencies, Foundations, and The University of Texas is acknowledged in footnotes to the appropriate sections.

METHODS OF MAGNETOTELLURIC ANALYSIS*

By

William E. Sims and F. X. Bostick, Jr.
Department of Electrical Engineering

Technical Report No. 58
January 7, 1969

ELECTRICAL GEOPHYSICS RESEARCH LABORATORY

prepared under

Grant GA-1236

National Science Foundation

and

Contract N00014-67-A-0216-0004

Office of Naval Research

Washington, D. C.

ELECTRONICS RESEARCH CENTER

THE UNIVERSITY OF TEXAS AT AUSTIN

Austin, Texas 78712

*Research sponsored in part by the Joint Services Electronics Program under the Research Grant AF-AFOSR-67-766E

ABSTRACT

Magnetotelluric prospecting is a method of geophysical exploration that makes use of the fluctuations in the natural electric and magnetic fields that surround the earth. These fields can be measured at the surface of the earth and they are related to each other by a surface impedance that is a function of the conductivity structure of the earth's substrata.

This report describes some new methods for analyzing and interpreting magnetotelluric data. A discussion is given of the forms of the surface impedance for various classes of models, including one, two and three dimensional models. Here, an n dimensional model is one in which the parameters describing the model are functions of at most n space coordinates. Methods are discussed for estimating the strike direction for data that is at least approximately two dimensional. A new linearized approach to the one dimensional problem is discussed. Subject to the approximations of the linearization, it is shown that under the appropriate transformations of the frequency and depth scales, the reciprocal of the surface impedance as a function of frequency is equal to the square root of the conductivity as a function of depth convolved with a linear response function that is somewhat like a low pass filter.

Included in this report is a comparison of several methods of estimating the auto and cross power density spectra of measured field data, and of several methods for estimating the surface impedance from these spectra. The effects of noise upon these estimates are considered in some detail. Special emphasis is given to several types of artificial noise including aliasing, round off or digitizer noise, and truncation effects. Truncation effects are of the most interest since they depend upon the particular window used in the spectral analysis.

TABLE OF CONTENTS

LIST OF FIGURES

I. INTRODUCTION

Magnetotelluric prospecting is a relatively new method of geophysical exploration, although the electric and magnetic fields that it employs have long been observed. More than a century ago it was recognized by several investigators that a correlation existed between the variations in the telluric currents and the geomagnetic field. In 1940 Chapman and Bartels reviewed the various theories on the relationship between these fields. In the late 1940's and early 1950's several investigators such as Tikhonov in the USSR; Kato, Kikuchi, Rikitake, and Yokoto in Japan; and Cagniard in France began to recognize the electromagnetic nature of these fields.

In 1953 Cagniard published a paper in which he gave a quantitative description of the relationship between the electric and magnetic fields at the surface of a horizontally layered earth. Soon thereafter many people began making theoretical and experimental contributions to the field of magnetotellurics. By the late 1950's, it was recognized by several investigators that the scalar impedance described by Cagniard was not sufficient to describe many of the frequently encountered geologic situations. For an anisotropic or laterally inhomogeneous earth, the impedance becomes a tensor quantity (Neves, 1957), (Rankin, 1960), (Cantwell, 1960), (Kovtun, 1961), (Rokityanskii, 1961), (d'Erceville and Kunetz, 1962), (Bostick and Smith, 1962), (Srivastava, 1963). Principal contributors to the growing body of literature on magnetotellurics, in addition to those previously mentioned, include Berdichevskii, Vladimirov, and Kolmakov in the USSR, Porstendorfer in Germany, Adam and Vero of the Hungarian Academy of Sciences, Fournier in France, and many people in the U.S.A. and Canada. Hugo Fournier (1966) has a comprehensive history and bibliography of the science of magnetotellurics.

The tensor relationship between the E (electric) and H (magnetic) fields at any given frequency can be expressed as

$$\begin{bmatrix} E_x \\ E_y \end{bmatrix} = \begin{bmatrix} Z_{xx} & Z_{xy} \\ Z_{yx} & Z_{yy} \end{bmatrix} \begin{bmatrix} H_x \\ H_y \end{bmatrix} \qquad (1.1)$$

where rectangular cartesian coordinates have been indicated. This tensor impedance Z, a function of frequency and space coordinates, depends upon the conductivity of the earth in the surrounding area, and if the horizontal wavelengths of the incident fields are sufficiently long, Z will be independent of time and source polarization. Therefore, Z can be a useful measure of the conductivity structure of the earth, and in fact it can sometimes be interpreted almost completely in terms of a simplified earth model.

The magnetotelluric problem can conveniently be divided into three parts: data acquisition, analysis, and modeling. Data acquisition includes the instrumentation and all of the field work involved with recording the electric and magnetic field variations. Analysis includes processing the field measurements to determine estimates of the Z tensor and other related parameters. Modeling consists of interpreting this impedance tensor in terms of a particular earth model.

The research that went into this thesis was aimed at developing better methods of magnetotelluric analysis and interpretation. The thesis itself provides for the first time a unified treatment of the techniques developed as a result of this research. The treatment is facilitated by first considering the forms of theoretical impedance tensors for several classes of models. Next, various methods are presented for estimating actual impedance tensors from measured field data. Finally, the effects that various types of noise have upon the impedance estimates are considered.

II. ONE DIMENSIONAL MODELS

In this chapter several one dimensional models, that is, models which have medium parameters that are functions of only one space coordinate will be considered.

A. Homogeneous Half Space Model

The simplest of all possible models is one in which the earth is considered to be a homogeneous, isotropic half space of conductivity σ, permittivity ϵ, permeability μ. Within any medium of constant σ, ϵ, and μ, if we assume time variations of the form $e^{j\omega t}$, Maxwell's equations

$$\nabla \times \vec{E} = - j\omega\mu \vec{H} \tag{2.1}$$

$$\nabla \times \vec{H} = (\sigma + j\omega\epsilon) \vec{E} \tag{2.2}$$

$$\nabla \cdot \vec{H} = 0 \tag{2.3}$$

$$\nabla \cdot \vec{E} = 0 \tag{2.4}$$

combine to give the vector Helmholtz equations

$$\nabla^2 \vec{E} = - \gamma^2 \vec{E}$$

$$\nabla^2 \vec{H} = - \gamma^2 \vec{H}$$

where

$$\gamma^2 = j\omega\mu\sigma - \omega^2\mu\epsilon \tag{2.5}$$

In rectangular cartesian coordinates, this vector equation separates, so that each of the components of the E and H fields satisfies the scalar Helmholtz equation. Elementary solutions to this equation are of the form

$$A\epsilon^{-(\gamma_x x + \gamma_y y + \gamma_z z)}$$

where

$$\gamma_x^2 + \gamma_y^2 + \gamma_z^2 = \gamma^2 = j\omega\mu\sigma - \omega^2\mu\epsilon \tag{2.6}$$

The general solution is obtained by summing various elementary solutions with different values of A, γ_x, γ_y, and γ_z, subject to the constraints of equation (2.6). Returning for the moment to an elementary solution, if the coordinate axes are aligned such that positive z is down, and the direction of propagation is in the x-z plane, then the elementary solution is of the form

$$Ae^{-\gamma_x x - \gamma_z z}\ ;\ \gamma_x^2 + \gamma_z^2 = \gamma^2 \tag{2.7}$$

Thus, for a homogeneous plane electromagnetic wave with its direction of propagation in the x-z plane, each of the components of E and H will be of the form shown in (2.7).

Since any homogeneous plane wave can be separated into TE (horizontal E field only) and TM (horizontal H field only) modes, and since the equations are linear with respect to the fields, one can consider the two modes separately.

For the TE mode,

$$E_x = E_z = 0$$

and equation (2.1) becomes

$$-\bar{i}\frac{\partial E_y}{\partial z} + \bar{k}\frac{\partial E_y}{\partial x} = -j\omega\mu(\bar{i}H_x + \bar{j}H_y + \bar{k}H_z)$$

Thus

$$\gamma_z E_y = -j\omega\mu H_x$$

$$-\gamma_x E_y = -j\omega\mu H_z$$

$$H_y = 0$$

In particular,

$$Z_{TE} = -\frac{E_y}{H_x} = \frac{j\omega\mu}{\gamma_z} \tag{2.8}$$

For the TM mode,

$$H_x = H_z = 0$$

and equation (2.2) becomes

$$-\bar{i}\frac{\partial H_y}{\partial z} + \bar{k}\frac{\partial H_y}{\partial x} = (\sigma + j\omega\epsilon)(\bar{i}E_x + \bar{j}E_y + \bar{k}E_z)$$

Thus

$$\gamma_z H_y = (\sigma + j\omega\epsilon) E_x$$

$$-\gamma_x H_y = (\sigma + j\omega\epsilon) E_z$$

$$E_y = 0$$

and

$$Z_{TM} = \frac{E_x}{H_y} = \frac{\gamma_z}{(\sigma + j\omega\epsilon)} = \frac{j\omega\mu\gamma_z}{\gamma^2} \tag{2.9}$$

For the range of parameters normally encountered in magnetotelluric work, displacement currents in the earth can be neglected. That is to say

$$\omega\epsilon << \sigma \tag{2.10}$$

so that

$$\gamma^2 = j\omega\mu\sigma \tag{2.11}$$

Continuity of the tangential fields at the surface z = 0 requires that

$$\gamma_{x\ air} = \gamma_{x\ earth} \tag{2.12}$$

For a plane wave striking the earth at a real angle θ measured from normal incidence,

$$\gamma_{x\ air} = j\omega\sqrt{\mu\epsilon}\ \sin\ \vartheta \tag{2.13}$$

Equation (2.10), (2.12) and (2.13) together imply that $|\gamma_x|^2 << |\gamma|^2$. Therefore one may take

$$\gamma_z = \gamma = \sqrt{j\omega\mu\sigma} \tag{2.14}$$

Under these conditions, equations (2.8) and (2.9) give

$$Z_{TE} = Z_{TM} = \sqrt{\frac{j\omega\mu}{\sigma}} \tag{2.15}$$

This implies that the impedance is independent of the polarization of the elementary solution. Thus, any general solution made up of elementary solutions satisfying the conditions of equation (2.14) will give a scalar impedance

$$Z = \sqrt{\frac{j\omega\mu}{\sigma}} \tag{2.16}$$

which will relate any horizontal component of the total H field to the orthogonal horizontal component of the E field.

Actually it is not necessary to restrict the general solution for the incident fields to modes corresponding to real angles of incidence, as

indicated by equation (2.13). Elementary solutions for which $|\gamma_x|^2 > \omega^2\mu\epsilon$ will still give rise to total fields which satisfy equation (2.16) provided

$$|\gamma_x|^2 << \omega\mu\sigma \tag{2.17}$$

It is convenient to define a parameter δ, called skin depth, for conductive materials by

$$\delta = \sqrt{2/\omega\mu\sigma} \tag{2.18}$$

Then

$$e^{-\gamma_z z} = e^{-(1+j)z/\delta} \tag{2.19}$$

Thus δ is a measure of the depth that an electromagnetic field will penetrate into a conductive medium. It is the depth at which the field will have been attenuated to 1/e of its surface value.

If one then defines the horizontal wavelength λ of an elementary solution by

$$\lambda = \frac{2\pi}{k_x}; \quad jk_x = \gamma_x$$

then a statement that is equivalent to equation (2.17) is that

$$\lambda >> \delta \tag{2.20}$$

In other words, the horizontal wavelength is long compared to the skin depth.

In summary then, for an earth model consisting of a homogeneous half space of conductivity σ, with incident fields having horizontal wavelengths long compared to a skin depth, the surface impedance will be given by equation (2.16).

B. Horizontally Layered Model

The next model that might be considered is one in which the earth is represented by a set of horizontal layers, each with a different conductivity. This is usually known as the Cagniard model since it is the one that he considered in his classic paper. One assumes N layers, as shown in figure 1, and assumes elementary solutions in each layer of the form

$$(A_i e^{-\gamma_{zi} z} + B_i e^{\gamma_{zi} z}) e^{-\gamma_{xi} x}$$

where

$$\gamma_{xi}^2 + \gamma_{zi}^2 = \gamma_i^2 = j\omega\mu\sigma_i \tag{2.21}$$

By requiring that the tangential fields be continuous at each boundary, and noting that $B_N = 0$ since the fields must vanish for large z, one finds that the impedance Z_i looking down from the top of the ith layer is given by

$$Z_i = Z_{oi} \frac{1 - R_i e^{-2\gamma_{zi} d_i}}{1 + R_i e^{-2\gamma_{zi} d_i}} ; \quad i = 1, 2, \ldots N-1$$

$$Z_N = Z_{oN} \tag{2.22}$$

where d_i is the thickness of the ith layer, R_i is a reflection coefficient defined by

$$R_i = \frac{Z_{oi} - Z_{i+1}}{Z_{oi} + Z_{i+1}} \qquad i = 1, 2, \ldots N-1 \tag{2.23}$$

and Z_{oi} is the characteristic impedance of the ith layer. As with the homogeneous half space, the characteristic impedance for the TE mode is

$$Z_{oi}^{TE} = j\omega\mu/\gamma_{zi} \tag{2.24}$$

and for the TM mode is

$$Z_{oi}^{TM} = j\omega\mu\ \gamma_{zi}/\gamma_i^2 \tag{2.25}$$

Again if one assumes that the horizontal wavelengths of the incident fields are long compared to a skin depth in each layer, the two modes become equivalent and

$$Z_{oi} = \sqrt{j\omega\mu/\sigma_i} \tag{2.26}$$

In either case, one may start at the bottom layer and work up, computing R_i and Z_i using the recursion equations (2.23) and (2.22) until Z_1, the surface impedance, is obtained.

Recall from equation (2.16) that for a homogeneous half space

$$\sigma = \frac{\omega\mu}{|Z|^2}$$

Correspondingly, for a layered model, it is customary to define an apparent conductivity $\sigma_a(\omega)$ or apparent resistivity $\rho_a(\omega)$ by

$$\sigma_a(\omega) = \frac{\omega\mu}{|Z_1(\omega)|^2} = \frac{1}{\rho_a(\omega)} \tag{2.27}$$

Some sample curves of apparent resistivity versus frequency for several models are plotted in figures 2 and 3. For high frequencies, $\sigma_a = \sigma_1$, and for low frequencies, $\sigma_a = \sigma_N$. Qualitatively it appears that $\sigma_a(\omega)$ is a "smoothed out" version of $\sigma(z)$ with frequency ω being inversely related to depth z.

Although it is a simple matter to obtain the surface impedance $Z_1(\omega)$ in terms of $\sigma(z)$ for any layered model, the inverse problem of finding $\sigma(z)$ for a specified $Z_1(\omega)$ is not so simple. It is a nonlinear problem that in general can be solved only by using iterative techniques. Computer programs are available for least squares fitting $Z(\omega)$ curves to N layer models (Patrick, 1969).

Since $\sigma_a(\omega)$ is a smooth curve, one might suspect that fine details in $\sigma(z)$ cannot be determined from $\sigma_a(\omega)$. This in fact turns out to be the case; only gross trends in $\sigma(z)$ can successfully be determined from $\sigma_a(\omega)$.

C. General One Dimensional Model

Consider the case where $\sigma(z)$ is a continuously varying function of z rather than being restricted to a finite number of homogeneour layers. In this case, the recursion equations (2.22) and (2.23) are replaced by a differential equation for Z. There are several ways to obtain the differential equation. One way is to combine the recursion equations (2.22) and (2.23), and let Δz replace d_i, and consider the limit as Δz approaches zero. Another simpler method pointed out by Swift (1967) uses Maxwell's equations directly. Consider the TE mode with $E_x = E_z = 0$. Equations (2.1) and (2.2) give

$$\frac{\partial E_y}{\partial z} = j\omega\mu H_x$$

$$\frac{\partial E_y}{\partial x} = -j\omega\mu H_z$$

$$\sigma E_y = -\frac{\partial H_z}{\partial x} + \frac{\partial H_x}{\partial z}$$

Now

$$Z_{TE} = - \frac{E_y}{H_x}$$

$$\frac{\partial Z_{TE}}{\partial z} = - \frac{1}{H_x} \frac{\partial E_y}{\partial z} + \frac{E_y}{H_x^2} \frac{\partial H_x}{\partial z}$$

$$= - \frac{1}{H_x} \left[j\omega\mu \, H_x \right] + \frac{E_y}{H_x^2} \left[\sigma E_y + \frac{\partial H_z}{\partial x} \right]$$

$$= - j\omega\mu + \frac{E_y}{H_x^2} \left[\sigma E_y - \frac{1}{j\omega\mu} \frac{\partial^2 E_y}{\partial x^2} \right]$$

$$= - j\omega\mu + \sigma Z_{TE}^2 - \frac{\gamma_x^2}{j\omega\mu} Z_{TE}^2$$

$$\frac{\partial Z_{TE}}{\partial z} = - j\omega\mu + (1 - \frac{\gamma_x^2}{\gamma^2}) \sigma Z_{TE}^2 \qquad (2.28)$$

Similarly for the TM mode one obtains

$$\frac{\partial Z_{TM}}{\partial z} = - j\omega\mu \, (1 - \frac{\gamma_x^2}{\gamma^2}) + \sigma Z_{TM}^2 \qquad (2.29)$$

Again when the incident fields have horizontal wavelengths large compared to a skin depth, the TE and TM modes become equivalent and

$$\frac{\partial Z}{\partial z} = - j\omega\mu + \sigma Z^2 \qquad (2.30)$$

This differential equation is of course nonlinear in Z; however, if one assumes a $\sigma(z)$ profile such that $\sigma(z) = \sigma_1$, a constant for $z > z_1$, then $Z(z_1) = \sqrt{j\omega\mu/\sigma_1}$ and equation (2.30) can be numerically integrated from $z = z_1$ to $z = 0$ to obtain an expression for the surface impedance in terms of the conductivity profile.

Thus, as with the layered model, the forward going problem of finding the surface impedance in terms of a specified conductivity profile is relatively simple. Again, the inverse problem of finding the $\sigma(z)$ profile which produces a specified surface impedance must be worked iteratively.

D. Linearized One Dimensional Model

Consider the following simplification of the one dimensional problem. Assume that the E field as a function of depth z has the form

$$E_x(z) = Ae^{-\int_0^z \gamma(z')\,dz'} \tag{2.31}$$

where A is independent of z and

$$\gamma(z) = \sqrt{j\omega\mu\,\sigma(z)} \tag{2.32}$$

From Maxwell's equations

$$\frac{dH_y}{dz} = -\sigma E_x$$

Integrating with respect to z and noting that H_y must vanish as $z \to \infty$, one has

$$\int_0^\infty \frac{dH_y}{dz}\,dz = -\int_0^\infty \sigma\, E_x\, dz$$

or

$$H_y(\infty) - H_y(o) = -\int_o^\infty \sigma(z)\, Ae^{-\int_o^z \gamma(z')\, dz'}\, dz$$

Thus, if one defines the surface admittance $Y(\omega)$ as being the reciprocal of the surface impedance, then

$$Y(\omega) = \frac{H_y(z=o)}{E_x(z=o)} = \int_o^\infty \sigma(z)\, e^{-\int_o^z \gamma(z')\, dz'}\, dz \qquad (2.33)$$

or, from equation (2.32)

$$Y(\omega) = \int_o^\infty \sigma(z)\, e^{-\sqrt{j\omega\mu}\int_o^z \sqrt{\sigma(z')}\, dz'}\, dz \qquad (2.34)$$

Now consider the following transformation. Let

$$e^{\alpha_1} = \int_o^z \sqrt{\sigma(z')}\, dz' \qquad (2.35)$$

and

$$e^{-\alpha_2} = \sqrt{\omega\mu/2} \qquad (2.36)$$

Noting that

$$e^{\alpha_1}\, d\alpha_1 = \sqrt{\sigma(z)}\, dz \qquad (2.37)$$

and

$$z = o \rightarrow \alpha_1 = -\infty$$

$$z = \infty \rightarrow \alpha_1 = \infty$$

equation (2.34) becomes

$$Y(\alpha_2) = \int_{-\infty}^{\infty} \sqrt{\sigma(\alpha_1)}\ e^{-(1+j)\, e^{(\alpha_1 - \alpha_2)}}\ e^{\alpha_1}\, d\alpha_1$$

or

$$Y(\alpha_2)\, e^{-\alpha_2} = \int_{-\infty}^{\infty} \sqrt{\sigma(\alpha_1)}\ e^{-(1+j)\, e^{-(\alpha_2 - \alpha_1)}}\ e^{-(\alpha_2 - \alpha_1)}\, d\alpha_1 \qquad (2.38)$$

Noting from equation (2.27) that

$$\sqrt{\sigma_a(\omega)} = \sqrt{\omega\mu}\ |Y(\omega)|$$

equation (2.38) gives

$$\sqrt{\sigma_a(\alpha)} = |\sqrt{\sigma(\alpha)} * g(\alpha)| \qquad (2.39)$$

where

$$g(\alpha) = \sqrt{2}\ e^{-(1+j)\, e^{-\alpha}}\ e^{-\alpha} \qquad (2.40)$$

Thus, under this simplified model, which in effect neglects internal reflections in the E field, the apparent conductivity can be obtained by convolving the actual conductivity profile with a complex linear response

function in α-space. A plot of the magnitude of $g(\alpha)$ versus α is shown in figure 4. The magnitude of $g(\alpha)$ peaks up at $\alpha = 0$ and decays as $|\alpha|$ increases. Also

$$\left| \int_{-\infty}^{\infty} g(\alpha)\, d\alpha \right| = 1$$

So $g(\alpha)$, although it is complex, is somewhat like the response of a low pass filter with unity DC gain. This is consistent with the earlier observation that $\sigma_a(\omega)$ is a "smoothed out" version of $\sigma(z)$ with ω inversely related to z.

In practice, this simplified approach is probably not very useful by itself since the assumed form of the E field in equation (2.31) is not too realistic. Strictly speaking it is valid only if

$$\left| \frac{d\sigma(z)}{dz} \right| << \gamma(z)\, \sigma(z) \tag{2.41}$$

for all z. On the other hand this approach could be quite useful for obtaining a first guess to be used in an iterative inversion scheme. In particular if one simply assumes that

$$\sigma(\alpha) \cong \sigma_a(\alpha) \tag{2.42}$$

then frequency and depth may be related through equations (2.35) and (2.36) to give

$$\sigma(z) \cong \sigma_a(z_a(\omega)) \tag{2.43}$$

where

$$z_a(\omega) = \int_{\omega}^{\infty} \frac{d\omega_o}{\sqrt{2\omega_o^3 \mu \sigma_a(\omega_o)}} \tag{2.44}$$

Thus, an approximate depth scale may be attached to the frequency scale for an apparent conductivity curve. Notice that for $\sigma_a(\omega) = \sigma$, a constant, equation (2.44) reduces to the standard skin depth, so one may think of $z_a(\omega)$ as sort of an integrated skin depth. In fact, for cases where equation (2.41) is satisfied, $z_a(\omega)$ will be the depth at which the fields have decayed to 1/e of their surface value.

E. Generalized Skin Depth

As suggested by the preceding paragraph, it will be useful to generalize the idea of skin depth for an inhomogeneous model. For a homogeneous medium, the skin depth was defined to be the depth at which the fields are attenuated to 1/e of their surface values. For an inhomogeneous model, the fields of course do not have a simple exponential decay; however, if one defines $\delta(\omega)$ to be the depth at which

$$\mathrm{Re}\left[\int_0^{\delta(\omega)} \sqrt{j\omega\mu\sigma(z)}\, dz\right] = 1 \tag{2.45}$$

then δ will be a good measure of the depth of penetration of the fields and as such it may be taken as the skin depth.

In the discussion of the horizontally layered model, the statement was made that the incident fields could be treated as normally incident plane waves if the actual horizontal wavelengths were long compared to a skin depth in each layer since for that case

$$Y_{zi} \cong Y_i$$

A less restrictive yet adequate requirement is that

$$\int_0^{\delta} Y_z\, dz \cong \int_0^{\delta} Y\, dz \tag{2.46}$$

where δ is defined by equation (2.45). Clearly this condition will exist provided

$$\left| \int_0^{\delta} \gamma_x \, dz \right| \ll \left| \int_0^{\delta} \gamma \, dz \right| \tag{2.47}$$

where $\gamma_x^2 + \gamma_z^2 = \gamma^2 = j\omega\mu\sigma$. But $\gamma_x = jk_x = j2\pi/\lambda$. Thus

$$\left| \int_0^{\delta} \gamma_x \, dz \right| = \frac{2\pi\delta}{\lambda} \tag{2.48}$$

Also, from equation (2.45), the definition of δ,

$$\left| \int_0^{\delta} \gamma \, dz \right| = \sqrt{2}$$

Thus, the condition (2.47) will exist provided

$$\frac{2\pi\delta}{\lambda} \ll \sqrt{2}$$

or

$$\delta \ll \lambda/\sqrt{2\pi}$$

So, if the horizontal wavelengths are long compared to the skin depth defined by equation (2.45), the incident fields may in effect be treated as normally incident plane waves.

In conclusion then, the forward going one dimensional problem is reasonably simple. If the incident fields are assumed to have horizontal wavelengths long compared to a skin depth, then any horizontal component of the H field is related to the orthogonal horizontal component of the E

field by a scalar impedance which is related to the conductivity profile. The inverse problem of estimating the conductivity profile from a measured surface impedance, while it is nonlinear has been worked with some success using iterative techniques. The simple linearized model discussed here should be useful for providing a first guess for such iterative solutions.

III. TWO AND THREE DIMENSIONAL MODELS

The scalar surface impedance discussed in the previous chapter is not sufficient to describe the relationship between the horizontal E and H fields for a model that has lateral variations in conductivity. In this chaper some general relationships will be developed for two dimensional models (models for which σ is a function of two space coordinates, the vertical or z coordinate and one horizontal coordinate, say x) and for three dimensional models (models for which σ is a function of all three space coordinates). It will be shown that for these models the impedance must be expressed as a rank two tensor as was indicated in equation (1.1).

A. Z_{TE} and Z_{TM} for Two Dimensional Models

Consider again Maxwell's equations as stated in equations (2.1) through (2.4). If one assumes that the conductivity σ is a function of x and z, equations (2.1) through (2.3) are still applicable; however, equation (2.4) must be replaced by

$$\nabla \cdot (\sigma E) = 0 \tag{3.1}$$

where once again it is assumed that displacement currents in the earth are negligible. If one also assumes once again that the horizontal wavelengths of the incident fields are long compared to a skin depth, then in the earth, everything is essentially uniform in the y direction so that equations (2.1) through (2.3) together with equation (3.1) in component form become

$$-\frac{\partial E_y}{\partial z} = -j\omega\mu H_x \tag{3.2}$$

$$\frac{\partial E_x}{\partial z} - \frac{\partial E_z}{\partial x} = -j\omega\mu H_y \tag{3.3}$$

$$\frac{\partial E_y}{\partial x} = j\omega\mu H_z \tag{3.4}$$

$$-\frac{\partial H_y}{\partial z} = \sigma E_x \tag{3.5}$$

$$\frac{\partial H_x}{\partial z} - \frac{\partial H_z}{\partial x} = \sigma E_y \tag{3.6}$$

$$\frac{\partial H_y}{\partial x} = \sigma E_z \tag{3.7}$$

$$\frac{\partial H_x}{\partial x} + \frac{\partial H_z}{\partial z} = 0 \tag{3.8}$$

$$\frac{\partial(\sigma E_x)}{\partial x} + \frac{\partial(\sigma E_z)}{\partial z} = 0 \tag{3.9}$$

Observe that the only field components involved in equations (3.2), (3.4), (3.6), and (3.8) are E_y, H_x, and H_z. Also, the only components entering equations (3.3), (3.5), (3.7), and (3.9) are E_x, E_z, and H_y. Thus it is apparent that the two modes are decoupled and may be considered separately. The mode involving E_y, H_x, and H_z is usually called the TE or E parallel mode since the E field is horizontal and parallel to the strike. The mode involving E_x, E_z, and H_y is called the TM or E perpendicular mode since the magnetic field is horizontal and the electric field is perpendicular to the strike. The strike is the direction along which there are no variations in the model parameters, in this case, the y direction.

Thus, for a two-dimensional model two impedances are required to define the relationship between the horizontal components of the E and H fields: $Z_{TE} = -E_y/H_x$ and $Z_{TM} = E_x/H_y$. Exact solutions for $Z_{TE}(\omega,x)$ and $Z_{TM}(\omega,x)$ in terms of $\sigma(x,z)$ are not tractable analytically although a few approximate cases have been worked out. In general, solutions are obtainable only by using numerical methods such as finite differencing over a two dimensional grid. Computer programs are available which implement these

techniques (Patrick, 1969). It would appear that the inverse problem of finding $\sigma(x,z)$ in terms of $Z_{TE}(\omega,x)$ and $Z_{TM}(\omega,x)$ could in principle be solved using iterative techniques similar to those used for the one dimensional inverse problem. It is believed that such a solution would be unique, although no proof is known. On the other hand, the number of calculations involved for grids large enough to be of interest is so great that the problem seems to be out of the range of present day computers. Nevertheless, useful and instructive information about two dimensional modeling can be obtained from solutions of the forward going problem.

B. Z in a General Coordinate System for Two Dimensional Models

As was shown above, for a two dimensional model the TE and TM modes decouple when one of the horizontal coordinates is aligned with the strike. It will now be useful to obtain the relationship between the tangential fields in a coordinate system in which the horizontal axes are arbitrarily oriented.

Suppose that the x' - y' coordinate system as shown in figure 5 is aligned with the strike, so that

$$E'_x = Z_{TM} H'_y \tag{3.10}$$

and

$$E'_y = -Z_{TE} H'_x \tag{3.11}$$

Suppose that the x-y coordinate system is oriented at an angle θ with respect to the x' - y' system as shown in figure 5. Then

$$E_x = E'_x \cos\theta + E'_y \sin\theta \tag{3.12}$$

$$E_y = -E'_x \sin\theta + E'_y \cos\theta \tag{3.13}$$

and

$$H_x = H'_x \cos\theta + H'_y \sin\theta \tag{3.14}$$

$$H_y = -H'_x \sin\theta + H'_y \cos\theta \tag{3.15}$$

or alternately

$$H'_x = H_x \cos\theta - H_y \sin\theta \tag{3.16}$$

$$H'_y = H_x \sin\theta + H_y \cos\theta \tag{3.17}$$

Combining these equations gives

$$\begin{aligned} E_x &= E'_x \cos\theta + E'_y \sin\theta \\ &= (Z_{TM} H'_y) \cos\theta + (-Z_{TE} H'_x) \sin\theta \\ &= Z_{TM}(H_x \sin\theta + H_y \cos\theta)\cos\theta - Z_{TE}(H_x \cos\theta - \\ &\qquad - H_y \sin\theta) \sin\theta \\ &= H_x[(Z_{TM} - Z_{TE}) \sin\theta \cos\theta] + H_y[Z_{TM} \cos^2\theta + \\ &\qquad + Z_{TE} \sin^2\theta] \end{aligned}$$

Thus if one defines

$$E_x = Z_{xx} H_x + Z_{xy} H_y$$

then

$$\begin{aligned} Z_{xx} &= (Z_{TM} - Z_{TE}) \sin\theta \cos\theta \\ &= \left(\frac{Z_{TM} - Z_{TE}}{2}\right) \sin 2\theta \end{aligned}$$

and

$$\begin{aligned} Z_{xy} &= Z_{TM} \cos^2\theta + Z_{TE} \sin^2\theta \\ &= \left(\frac{Z_{TM} + Z_{TE}}{2}\right) + \left(\frac{Z_{TM} - Z_{TE}}{2}\right) \cos 2\theta \end{aligned}$$

Similarly for the other components, one obtains

$$Z_{yx} = -\left(\frac{Z_{TM} + Z_{TE}}{2}\right) + \left(\frac{Z_{TM} - Z_{TE}}{2}\right) \cos 2\theta$$

and

$$Z_{yy} = \left(\frac{Z_{TE} - Z_{TM}}{2}\right) \sin 2\theta$$

In summary

$$\begin{bmatrix} E_x \\ E_y \end{bmatrix} = \begin{bmatrix} Z_1 \sin 2\theta & Z_2 + Z_1 \cos 2\theta \\ -Z_2 + Z_1 \cos 2\theta & -Z_1 \sin 2\theta \end{bmatrix} \begin{bmatrix} H_x \\ H_y \end{bmatrix} \tag{3.18}$$

where

$$Z_1 = (Z_{TM} - Z_{TE})/2 \tag{3.19}$$

$$Z_2 = (Z_{TM} + Z_{TE})/2 \tag{3.20}$$

In general, then, for a two dimensional model, the tangential components of E and H are related by a rank two tensor impedance. The diagonal terms of the Z matrix are in general negatives of each other and they reduce to zero when the axes are aligned with the strike.

C. General Form of Z for Three Dimensional Models

For three dimensional models where σ is a function of all three space coordinates, the six field components are in general all coupled to each other, so it is not possible to separate the analysis into two distinct modes as was done for the two dimensional case. Nevertheless, it is possible to make some general statements about the relationship between the tangential components of the E and H fields.

It will now be shown that a rank two tensor impedance of the form shown in equation (1.1) is unique and stable, subject once again of course to the assumption that the horizontal wavelengths of the incident fields are long compared to a skin depth in the earth. Also it will be useful for later purposes to establish that in general the vertical magnetic field can be expressed as a linear combination of the two horizontal H field components. That is,

$$H_z = r_{zx} H_x + r_{zy} H_y \tag{3.21}$$

where r_{zx} and r_{zy} are dimensionless constants, subject also of course to the assumption that the incident fields have horizontal wavelengths long compared to a skin depth. This assumption implies that the incident fields may be treated as normally incident plane waves. This being the case, the incident fields can be separated into two orthogonal linearly polarized plane waves. Clearly, for a linearly polarized normally incident plane wave, each of the components of the total E and H fields will be proportional to the amplitude of the incident wave. Thus, if the incident E is linearly polarized in the x direction then

$$E_x = a_1 E_{xi}$$

$$E_y = a_2 E_{xi}$$

$$H_x = b_1 E_{xi}$$

$$H_y = b_2 E_{xi}$$

$$H_z = c_1 E_{xi}$$

where E_{xi} is the incident field. Similarly, if the incident E is linearly polarized in the y direction

$$E_x = a_3 E_{yi}$$

$$E_y = a_4 E_{yi}$$

$$H_x = b_3 E_{yi}$$

$$H_y = b_4 E_{yi}$$

$$H_z = c_2 E_{yi}$$

Since all of the field equations are linear with respect to E and H, superposition must hold. Thus for a general normally incident plane wave

$$E_x = a_1 E_{xi} + a_3 E_{yi}$$

$$E_y = a_2 E_{xi} + a_4 E_{yi}$$

$$H_x = b_1 E_{xi} + b_3 E_{yi}$$

$$H_y = b_2 E_{xi} + b_4 E_{yi}$$

$$H_z = c_1 E_{xi} + c_2 E_{yi}$$

or in matrix notation

$$\begin{bmatrix} E_x \\ E_y \end{bmatrix} = [A] \begin{bmatrix} E_{xi} \\ E_{yi} \end{bmatrix}$$

$$\begin{bmatrix} H_x \\ H_y \end{bmatrix} = [B] \begin{bmatrix} E_{xi} \\ E_{yi} \end{bmatrix}$$

and

$$H_z = [C] \begin{bmatrix} E_{xi} \\ E_{yi} \end{bmatrix}$$

If [B] is nonsingular, then

$$\begin{bmatrix} E_{xi} \\ E_{yi} \end{bmatrix} = [B]^{-1} \begin{bmatrix} H_x \\ H_y \end{bmatrix}$$

so that

$$\begin{bmatrix} E_x \\ E_y \end{bmatrix} = [A][B]^{-1} \begin{bmatrix} H_x \\ H_y \end{bmatrix}$$

and

$$H_z = [C][B]^{-1} \begin{bmatrix} H_x \\ H_y \end{bmatrix} \tag{3.22}$$

Thus

$$[Z] = [A][B]^{-1} \tag{3.23}$$

and

$$[r] = [r_{zx}, r_{zy}] = [C][B]^{-1} \tag{3.24}$$

So [Z] and [r] are defined, and E_x, E_y and H_z can be expressed as linear combinations of H_x and H_y. The only problem that might arise would be if [B] were singular. Singularity of [B] implies that

$$b_1 b_4 = b_2 b_3 \tag{3.25}$$

Now for any reasonable earth model, the reflection coefficient for the magnetic field at the surface is almost unity so that the total H field is close to twice the incident field. Thus, a normally incident plane wave with E linearly polarized in the x direction (and hence H linearly polarized in the y direction) will give rise to total fields such that H_y will be considerably greater than H_x. Thus

$$|b_2| >> |b_1|$$

Similarly, for a normally incident plane wave with E linearly polarized in the y direction, H_x will be somewhat greater than H_y. Thus

$$|b_3| >> |b_4|$$

So clearly

$$|b_2 b_3| >> |b_1 b_4|$$

Comparing this with equation (3.25) indicates that for any reasonable earth model, [B] will not be singular, and hence Z is defined by equation (3.23).

Next it will be useful to observe the behavior of the elements of Z as the coordinate system is rotated. As with the two dimensional model,

the elements of Z in the x-y coordinate system will be expressed in terms of the elements of Z in the x'-y' coordinate system as shown in figure 5. The derivation is the same as for the two dimensional case except that equations (3.10) and (3.11) are replaced by

$$E'_x = Z'_{xx} H'_x + Z'_{xy} H'_y \tag{3.26}$$

and

$$E'_y = Z'_{yx} H'_x + Z'_{yy} H'_y \tag{3.27}$$

Thus

$$\begin{aligned} E_x &= E'_x \cos\theta + E'_y \sin\theta \\ &= (Z'_{xx} H'_x + Z'_{xy} H'_y) \cos\theta + (Z'_{yx} H'_x + Z'_{yy} H'_y) \sin\theta \\ &= (Z'_{xx} \cos\theta + Z'_{yx} \sin\theta) H'_x + (Z'_{xy} \cos\theta + Z'_{yy} \sin\theta) H'_y \\ &= (Z'_{xx} \cos\theta + Z'_{yx} \sin\theta)(H_x \cos\theta - H_y \sin\theta) \\ &\quad + (Z'_{xy} \cos\theta + Z'_{yy} \sin\theta)(H_x \sin\theta + H_y \cos\theta) \\ &= [Z'_{xx} \cos^2\theta + Z'_{yy} \sin^2\theta + (Z'_{yx} + Z'_{xy}) \sin\theta \cos\theta] H_x \\ &\quad + [Z'_{xy} \cos^2\theta - Z'_{yx} \sin^2\theta + (Z'_{yy} - Z'_{xx}) \sin\theta \cos\theta] H_y \end{aligned}$$

So that

$$\begin{aligned} Z_{xx} &= Z'_{xx} \cos^2\theta + Z'_{yy} \sin^2\theta + (Z'_{xy} + Z'_{yx}) \sin\theta \cos\theta \\ &\left(\frac{Z'_{xx} + Z'_{yy}}{2}\right) + \left(\frac{Z'_{xx} - Z'_{yy}}{2}\right) \cos 2\theta + \left(\frac{Z'_{xy} + Z'_{yx}}{2}\right) \sin 2\theta \end{aligned}$$

Similar expressions for Z_{xy}, Z_{yx}, and Z_{yy} are obtained. The results are

$$Z_{xx} = Z_1 + Z_2 \cos 2\theta + Z_3 \sin 2\theta \tag{3.28}$$

$$Z_{xy} = Z_4 + Z_3 \cos 2\theta - Z_2 \sin 2\theta \tag{3.29}$$

$$Z_{yx} = -Z_4 + Z_3 \cos 2\theta - Z_2 \sin 2\theta \tag{3.30}$$

$$Z_{yy} = Z_1 - Z_2 \cos 2\theta - Z_3 \sin 2\theta \tag{3.31}$$

where

$$Z_1 = \frac{Z'_{xx} + Z'_{yy}}{2} \tag{3.32}$$

$$Z_2 = \frac{Z'_{xx} - Z'_{yy}}{2} \tag{3.33}$$

$$Z_3 = \frac{Z'_{xy} + Z'_{yx}}{2} \tag{3.34}$$

$$Z_4 = \frac{Z'_{xy} - Z'_{yx}}{2} \tag{3.35}$$

If one further defines

$$Z_o(\theta) = Z_3 \cos 2\theta - Z_2 \sin 2\theta \tag{3.36}$$

Then equations (3.28) through (3.31) become

$$Z_{xx} = Z_1 - Z_o(\theta + 45^\circ) \tag{3.37}$$

$$Z_{xy} = Z_4 + Z_o(\theta) \tag{3.38}$$

$$Z_{yx} = -Z_4 + Z_o(\theta) \tag{3.39}$$

$$Z_{yy} = Z_1 + Z_o(\theta + 45^\circ) \tag{3.40}$$

The function $Z_o(\theta)$ traces an ellipse in the complex plane centered on the origin as θ varies from zero to 180°. To show that this is true take

$$Z_o(\theta) = x + jy$$

where x and y are real. From equation (3.36)

$$x = \mathrm{Re}[Z_3]\cos 2\theta - \mathrm{Re}[Z_2]\sin 2\theta$$

$$= A\cos(2\theta - \alpha)$$

$$y = \mathrm{Im}[Z_3]\cos 2\theta - \mathrm{Im}[Z_2]\sin 2\theta$$

$$= B\cos(2\theta - \beta)$$

Letting

$$2\theta - \alpha = \varphi$$

$$\beta - \alpha = \varphi_o$$

gives

$$x = A\cos\varphi$$

and

$$y = B\cos(\varphi - \varphi_o) = C\cos\varphi + D\sin\varphi$$

Thus

$$\cos\varphi = \frac{x}{A}$$

and

$$\sin\varphi = \pm\sqrt{1 - (x/A)^2}$$

So that

$$y = C\left[\frac{x}{A}\right] + D\left[\pm\sqrt{1 - (x/A)^2}\right]$$

or

$$y^2 - \frac{2C}{A}xy + \frac{C^2}{A^2}x^2 = D^2\left(1 - \frac{x^2}{A^2}\right)$$

or

$$A^2y^2 + (C^2 + D^2)x^2 - 2ACxy - D^2A^2 = 0$$

This is the standard form for an ellipse centered on the origin. Thus $Z_o(\theta)$ traces an ellipse in the complex plane as θ varies. Referring to equations (3.37) through (3.40) one observes that each of the elements of Z then traces an ellipse in the complex plane as the measuring axes are rotated.

D. Comparison of Z Matrix for Two and Three Dimensional Models

As was shown in the previous section, for a three dimensional model, the elements of Z trace ellipses in the complex plane as the measuring axes are rotated. From equation (3.18) one observes that for two dimensional models, the theta dependent parts of the elements of Z have fixed phases. Thus the ellipses degenerate to straight lines for the two dimensional case. Also one observes from equation (3.18) that the diagonal terms of the Z matrix for the two dimensional case have no constant term. Thus the straight line representing the locii of Z_{xx} and Z_{yy} in the complex plane passes through the origin. Figure 6 illustrates the general form of the locii of the elements of Z in the complex plane for the two and three dimensional cases.

At the present time solutions for the general three dimensional problem are not available. For this reason, it is usually desirable to find one dimensional or two dimensional models that approximately fit measured data which in general is of course three dimensional. It frequently happens that, over some limited frequency range, measured data looks almost two dimensional; that is, the Z ellipses almost collapse to straight lines and the diagonal terms of the Z matrix are almost negatives of each other. This situation will occur whenever there exists a horizontal direction along which the conductivity cross section is nearly constant for a distance of several skin depths Whenever this situation exists, it is desirable to determine the approximate strike direction and to estimate the corresponding Z_{TE} and Z_{TM} for comparison with theoretical Z's from two dimensional models.

Several methods have been proposed for estimating the principal impedance axes [Swift, 1967] all of which converge to the correct result when the data is actually two dimensional. From the point of view of the impedance ellipses, the most reasonable way seems to be to take

$$Z_{TE}\ ,\ Z_{TM} = Z_4 \pm Z'_o \tag{3.41}$$

where Z'_o is the semi-major axis of the ellipse $Z_o(\theta)$ as defined in equation (3.36)

This method yields the principal directions as the values of θ which maximize $|Z_o(\theta)|$. A little algebra will show that these values of θ are given by the equation

$$\tan 4\theta = \frac{2(x_2x_3 + y_2y_3)}{(x_2^2 + y_2^2) - (x_3^2 + y_3^2)} \tag{3.42}$$

where x_i and y_i are the real and imaginary parts of Z_i respectively, with Z_i being defined by equations (3.33) and (3.34). Incidentally, this method gives the same result as Swift's method of finding the angle θ which maximizes $\{|Z_{xy}|^2 + |Z_{yx}|^2\}$ or minimizes $\{|Z_{xx}|^2 + |Z_{yy}|^2\}$.

Having thus obtained estimates of the principal axes of the impedance matrix and the corresponding principal impedance values, it is desirable to have some measure of how two dimensional the data actually is. To accomplish this, there are two parameters that should be considered. First, there is the ratio of the constant terms in the diagonal and off diagonal elements of the Z matrix. In other words, the ratio Z_1/Z_4 where Z_1 and Z_4 are defined in equations (3.32) and (3.35). Second, there is the ratio of the minor axis to the major axis of the $Z_o(\theta)$ ellipse. The magnitudes of both of these ratios should be small compared to unity in order for the data to fit a two dimensional model.

E. Use of H_z for Determining the Strike Direction

In the previous section, an indication was given as to how one might estimate the principal axes of a measured impedance matrix which is approximately two dimensional. However, no method was given for determining which axis represents the strike direction. This matter can be easily resolved in terms of H_z, the vertical magnetic field. Recall from equations (3.2) through (3.9) that H_z appears only in the equations for the TE mode. Thus, with the x'-y' axes aligned with the strike, as in section B of this chapter

$$E'_y = -Z_{TE} H'_x$$

and

$$H'_z = r'_{TE} H'_x$$

In the x-y coordinate system, at an angle θ from the x'-y' system

$$H_z = H'_z = r'_{TE} H'_x = r'_{TE} (H_x \cos\theta - H_y \sin\theta)$$

$$H_z = H_x r'_{TE} \cos\theta - H_y r'_{TE} \sin\theta \qquad (3.43)$$

Recall from equation (3.21) that for the general three dimensional model

$$H'_z = r'_{zx} H'_x + r'_{zy} H'_y$$

so that

$$H_z = H'_z = r'_{zx} H'_x + r'_{zy} H'_y$$

$$= r'_{zx} (H_x \cos\theta - H_y \sin\theta) + r'_{zy} (H_x \sin\theta + H_y \cos\theta)$$

$$= H_x (r'_{zx} \cos\theta + r'_{zy} \sin\theta) + H_y (r'_{zy} \cos\theta - r'_{zx} \sin\theta)$$

Thus

$$r_{zx} = r'_{zx} \cos\theta + r'_{zy} \sin\theta \qquad (3.44)$$

and

$$r_{zy} = r'_{zy} \cos\theta - r'_{zx} \sin\theta \qquad (3.45)$$

Comparison of equations (3.44) and (3.45) with equation (3.36) indicates that r_{zx} and r_{zy} like $Z_o(\theta)$ trace ellipses in the complex plane as θ varies. However, the important difference is that the magnitudes of r_{zx} and r_{zy} have only one peak every 180^o instead of every 90^o like $Z_o(\theta)$. Furthermore, one observes from equation (3.43) that in the two dimensional limit, the angle θ that maximizes r_{zx} is the strike direction.

Thus, when measured data is approximately two dimensional, the angle that maximizes $|r_{zx}|$ should correspond to one of the principal axes of

the Z matrix, and so it is possible to estimate the approximate strike direction and the corresponding Z_{TE} and Z_{TM}.

IV. METHODS FOR ESTIMATING THE Z MATRIX FROM MEASURED DATA

Now that a considerable amount of attention has been given to the forms of the Z matrix for various classes of models and to possible interpretations of Z, it is time to consider some methods for estimating Z from measured E and H field data.

A. The General Problem

Consider the equation

$$E_x = Z_{xx}H_x + Z_{xy}H_y$$

where E_x, H_x, and H_y may be considered to be Fourier transforms of measured electric and magnetic field data. If one has two independent measurements of E_x, H_x, and H_y at a given frequency, denoted by E_{x1}, H_{x1}, H_{y1}, E_{x2}, H_{x2} and H_{y2} respectively, then

$$Z_{xx} = \frac{\begin{vmatrix} E_{x1} & H_{y1} \\ E_{x2} & H_{y2} \end{vmatrix}}{\begin{vmatrix} H_{x1} & H_{y1} \\ H_{x2} & H_{y2} \end{vmatrix}}$$

and

$$Z_{xy} = \frac{\begin{vmatrix} H_{x1} & E_{x1} \\ H_{x2} & E_{x2} \end{vmatrix}}{\begin{vmatrix} H_{x1} & H_{y1} \\ H_{x2} & H_{y2} \end{vmatrix}}$$

provided

$$H_{x1}H_{y2} - H_{x2}H_{y1} \neq 0 \qquad (4.1)$$

Equation (4.1) simply states the fact that the two field measurements must have different source polarizations. If the two have the same polarization, they are not independent.

Since any physical measurement of E or H will include some noise, it is usually desirable to make more than two independent measurements, and then to use some type of averaging that will reduce the effects of the noise. Suppose one has n measurements of E_x, H_x, and H_y at a given frequency. One can then estimate Z_{xx} and Z_{xy} in the mean square sense. That is, define

$$\Psi = \sum_{i=1}^{n} (E_{xi} - Z_{xx}H_{xi} - Z_{xy}H_{yi})(E_{xi}^* - Z_{xx}^*H_{xi}^* - Z_{xy}^*H_{yi}^*)$$

where E_{xi}^* is the complex conjugate of E_{xi}, etc., and then find the values of Z_{xx} and Z_{xy} that minimize Ψ. Setting the derivatives of Ψ with respect to the real and imaginary parts of Z_{xx} to zero yields

$$\sum_{i=1}^{n} E_{xi}H_{xi}^* = Z_{xx} \sum_{i=1}^{n} H_{xi}H_{xi}^* + Z_{xy} \sum_{i=1}^{n} H_{yi}H_{xi}^* \qquad (4.2)$$

Similarly, setting the derivatives of Ψ with respect to the real and imaginary parts of Z_{xy} to zero yields

$$\sum_{i=1}^{n} E_{xi}H_{yi}^* = Z_{xx} \sum_{i=1}^{n} H_{xi}H_{yi}^* + Z_{xy} \sum_{i=1}^{n} H_{yi}H_{yi}^* \qquad (4.3)$$

Notice that the summations represent auto and cross power density spectra. Equations (4.2) and (4.3) may then be solved simultaneously for Z_{xx} and Z_{xy}. This solution will minimize the error caused by noise on E_x. It is possible to define other mean square estimates that minimize other types of noise. For example, if one takes

$$\Psi = \sum_{i=1}^{n} \left(\frac{E_{xi}}{Z_{xx}} - H_{xi} - \frac{Z_{xy}}{Z_{xx}} H_{yi}\right)\left(\frac{E^*_{xi}}{Z^*_{xx}} - H^*_{xi} - \frac{Z^*_{xy}}{Z^*_{xx}} H^*_{yi}\right)$$

the resulting solution will minimize the error introduced by noise on H_x.

There are four distinct equations that arise from the various mean square estimates. In terms of the auto and cross power density spectra, they are

$$\overline{E_x E^*_x} = Z_{xx}\overline{H_x E^*_x} + Z_{xy}\overline{H_y E^*_x} \tag{4.4}$$

$$\overline{E_x E^*_y} = Z_{xx}\overline{H_x E^*_y} + Z_{xy}\overline{H_y E^*_y} \tag{4.5}$$

$$\overline{E_x H^*_x} = Z_{xx}\overline{H_x H^*_x} + Z_{xy}\overline{H_y H^*_x} \tag{4.6}$$

and

$$\overline{E_x H^*_y} = Z_{xx}\overline{H_x H^*_y} + Z_{xy}\overline{H_y H^*_y} \tag{4.7}$$

Strictly speaking, equations (4.4) through (4.7) are valid only if $\overline{E_x E^*_x}$, $\overline{E_x E^*_y}$, etc. represent the power density spectra at a discrete frequency ω. In practice however, Z_{ij} are slowly varying functions of frequency, and as such, $\overline{E_x E^*_x}$, etc. may be taken as averages over some finite bandwidth. This is fortunate since it facilitates the estimation of the power density spectra.

B. Estimation of Power Density Spectra

There are a variety of standard techniques available for estimating $\overline{E_x E^*_x}$, $\overline{E_x E^*_y}$, etc., the auto and cross power density spectra, several of which will be considered here. In all the cases, it will be assumed that the field components are given as sampled time sequences.

1. One method that was frequently used in the past was that of using the auto and cross correlation functions of the field components. This method makes use of the fact that the Fourier transform of the auto correlation function of a given signal is equal to the power density spectrum of that signal. Also the Fourier transform of the cross correlation function between two signals is equal to the cross power density spectrum of the two signals. Blackman and Tukey (1958) have considered in detail the various aspects of estimating correlation functions and the corresponding power density spectra for sampled time sequences. They have given careful attention to the spectral windows that result from truncating the time sequences and the correlation functions. Hopkins (1966) and others have used this method for obtaining estimates of $\overline{E_x E_x^*}$, $\overline{E_x E_y^*}$, etc. in magnetotelluric work. This method, when compared with the ones that will be considered next, has several disadvantages. First it is more time consuming on the computer when many cross spectra are needed. Second, it gives statistically correct results only when the signals are stationary. Finally, it is more susceptible to error from the side lobes of the spectral window when the spectra are not reasonably flat. Blackman and Tukey suggest that this third disadvantage can be circumvented to some extent by digitally prewhitening the time sequences prior to computing the correlation functions.

2. Another method for estimating the power density spectra of the field components begins by subdividing each of the time sequences into several blocks. For each data block one computes the Fourier transformation to obtain estimates of $E_x(\omega)$, $E_y(\omega)$, etc. Then one forms the products $E_x E_x^*$, $E_x E_y^*$, etc. Finally, for each frequency, one averages the products over the several time blocks, thus obtaining time averaged estimates of $\overline{E_x E_x^*}$, $\overline{E_x E_y^*}$, $\overline{E_x H_x^*}$, etc. This method is particularly well suited to small digital computers since only one time block of data needs to be stored in memory at any given time, and the blocks may be quite small compared to the

total time sequences. Also this method is especially useful for situations where the signals contain noise bursts that are isolated in time. Such noise bursts may arise from tape drop-out, system saturation caused by large amplitude signals, or many other sources. Such noise bursts are often readily detectable so that data blocks containing them may simply be omitted from the time average.

3. Another method for estimating the power spectra that is very similar to the previous one consists of feeding the original time sequences into a bank of narrow band digital recursive filters spanning the desired frequency range. The outputs of these filters are then treated the same as the outputs of the block Fourier transforms of the previous method. This recursive filter method has essentially the same advantages as the previous method together with the additional advantage that it lends itself quite readily to obtaining spectral estimates equally spaced on a log frequency scale. This is because the recursive filters may be designed such that they all have the same Q and have the appropriate spacing on the frequency scale. Swift (1967) has used this technique.

4. For the final method to be considered here, one begins by Fourier transforming each of the entire time sequences. The products $E_x E_x^*$, $E_x E_y^*$, etc. are then formed for each harmonic. Finally the products are averaged over several neighboring harmonics to obtain the desired bandwidth. As far as computation time is concerned, this method is quite efficient if one uses the Cooley-Tukey algorithm for fast Fourier transforms. In fact, for a given number of multiplications, the spectral windows obtainable by this method are better than those obtainable by any of the other methods considered here. (A detailed discussion of spectral windows is included in Chapter V.) This method, like the last one, lends itself readily to constant Q estimates of the spectral density since the number of harmonics averaged in each band may be made approximately proportional to the center

frequency of the band. The primary disadvantage of this method is that, compared to the two previous methods, it requires a fairly large number of storage locations; in general it requires a large computer. Actually, in a modified form which is not quite as efficient computationally, the Cooley-Tukey algorithm is applicable to small computers. For a detailed consideration of this algorithm, see Cooley (1965).

If then, by one means or another, estimates of the auto and cross power density spectra are obtained, one can proceed to estimate the elements of the Z matrix.

C. Estimation of Z from Auto and Cross Power Density Spectra

Consider equations (4.4) through (4.7). Under certain conditions, these equations are independent so that any two of them may be solved simultaneously for Z_{xx} and Z_{xy}. Since there are six possible distinct pairs of equations, there are six ways to estimate Z_{xx} and Z_{xy}. For example, the six estimates for Z_{xy} are

$$\bar{Z}_{xy} = \frac{(\overline{H_x E_x^*})(\overline{E_x E_y^*}) - (\overline{H_x E_y^*})(\overline{E_x E_x^*})}{(\overline{H_x E_x^*})(\overline{H_y E_y^*}) - (\overline{H_x E_y^*})(\overline{H_y E_x^*})} \tag{4.8}$$

$$\bar{Z}_{xy} = \frac{(\overline{H_x E_x^*})(\overline{E_x H_x^*}) - (\overline{H_x H_x^*})(\overline{E_x E_x^*})}{(\overline{H_x E_x^*})(\overline{H_y H_x^*}) - (\overline{H_x H_x^*})(\overline{H_y E_x^*})} \tag{4.9}$$

$$\bar{Z}_{xy} = \frac{(\overline{H_x E_x^*})(\overline{E_x H_y^*}) - (\overline{H_x H_y^*})(\overline{E_x E_x^*})}{(\overline{H_x E_x^*})(\overline{H_y H_y^*}) - (\overline{H_x H_y^*})(\overline{H_y E_x^*})} \tag{4.10}$$

$$\bar{Z}_{xy} = \frac{(\overline{H_x E_y^*})(\overline{E_x H_x^*}) - (\overline{H_x H_x^*})(\overline{E_x E_y^*})}{(\overline{H_x E_y^*})(\overline{H_y H_x^*}) - (\overline{H_x H_x^*})(\overline{H_y E_y^*})} \tag{4.11}$$

$$\bar{Z}_{xy} = \frac{(\overline{H_x E_y^*})(\overline{E_x H_y^*}) - (\overline{H_x H_y^*})(\overline{E_x E_y^*})}{(\overline{H_x E_y^*})(\overline{H_y H_y^*}) - (\overline{H_x H_y^*})(\overline{H_y E_y^*})} \tag{4.12}$$

and

$$\bar{Z}_{xy} = \frac{(\overline{H_x H_x^*})(\overline{E_x H_y^*}) - (\overline{H_x H_y^*})(\overline{E_x H_x^*})}{(\overline{H_x H_x^*})(\overline{H_y H_y^*}) - (\overline{H_x H_y^*})(\overline{H_y H_x^*})} \tag{4.13}$$

where $\bar{Z}_{xy}$ denotes a measured estimate of Z_{xy}.

It turns out that two of these expressions tend to be relatively unstable for the one dimensional case, particularly when the incident fields are unpolarized. For this case $\overline{E_x E_y^*}$, $\overline{E_x H_x^*}$, $\overline{E_y H_y^*}$, and $\overline{H_x H_y^*}$ tend toward zero, so that equations (4.10) and (4.11) become indeterminant. The other four expressions are quite stable and correctly predict $Z_{xy} = E_x/H_y$ for the one dimensional case, provided the incident fields are not highly polarized.

This same thing is true of the other three impedance elements Z_{xx}, Z_{yx}, and Z_{yy}. In each case there are six ways to estimate Z_{ij}, two of which are unstable for one dimensional models with unpolarized incident fields. Also in each case the other four estimates are quite stable for any reasonable earth model provided the incident fields are not highly polarized.

As was mentioned earlier, any physical measurement of E or H will necessarily contain some noise. It is desirable now to consider how such noise will affect the Z estimates defined above. Suppose that

$$E_x = E_{xs} + E_{xn} \tag{4.14}$$

$$E_y = E_{ys} + E_{yn} \tag{4.15}$$

$$H_x = H_{xs} + H_{xn} \tag{4.16}$$

$$H_y = H_{ys} + H_{yn} \tag{4.17}$$

where

$$\begin{bmatrix} E_{xs} \\ E_{ys} \end{bmatrix} = \begin{bmatrix} Z_{xx} & Z_{xy} \\ Z_{yx} & Z_{yy} \end{bmatrix} \begin{bmatrix} H_{xs} \\ H_{ys} \end{bmatrix}$$

and E_{xn}, E_{yn}, H_{xn} and H_{yn} are noise terms. If the noise terms are all zero, then the four stable estimates of each of the elements of Z are the same, and

$$\bar{Z}_{ij} = Z_{ij}$$

On the other hand, when the noise terms are nonzero, the four estimates are in general different.

Equation (4.13) for Z_{xy} corresponds to the one that Swift (1967) used. He showed that his estimates of Z_{ij} were biased down by random noise on the H signal, but were not affected by random noise on the E signal. Similar arguments for the four stable estimates defined above indicate that in each case, two of them are biased down by random noise on H and are not biased by random noise on E (for example, equations (4.12) and (4.13) for $\bar{Z}_{xy}$) while the other two are biased up by random noise on E and are not biased by random noise on H (for example, equations (4.8) and (4.9) for $\bar{Z}_{xy}$). The effects of the noise are most easily seen for the one dimensional model. For this model, if the incident fields are depolarized so that $\overline{E_x E_y^*}$, $\overline{E_x H_x^*}$, $\overline{E_y H_y^*}$, and $\overline{H_x H_y^*}$ tend to zero, then equations (4.8) and (4.9) for $\bar{Z}_{xy}$ reduce to

$$\bar{Z}_{xy} = \overline{E_x E_x^*} / \overline{H_y E_x^*} \tag{4.18}$$

Equations (4.12) and (4.13) reduce to

$$\bar{Z}_{xy} = \overline{E_x H_y^*} / \overline{H_y H_y^*} \tag{4.19}$$

If one assumes that E_x and H_y are given by equations (4.14) and (4.17) and the E_{yn} and H_{xn} are random and independent of the signals and of each other, then the expected values of the power density spectra are

$$\langle \overline{E_x E_x^*} \rangle = \langle \overline{E_{xs} E_{xs}^*} \rangle + \langle \overline{E_{xn} E_{xn}^*} \rangle$$

$$\langle \overline{H_y H_y^*} \rangle = \langle \overline{H_{ys} H_{ys}^*} \rangle + \langle \overline{H_{yn} H_{yn}^*} \rangle$$

$$\langle \overline{E_x H_y^*} \rangle = \langle \overline{H_y E_x^*} \rangle^* = \langle \overline{E_{xs} H_{ys}^*} \rangle$$

Thus, if the spectral estimates contain enough terms in the average so that the cross terms may be neglected (i.e. $\overline{E_{xs} E_{xn}^*}$, etc. are negligible), then equation (4.18) gives

$$\bar{Z}_{xy} = \frac{\overline{E_{xs} E_{xs}^*} + \overline{E_{xn} E_{xn}^*}}{\overline{H_{ys} E_{xs}^*}} = Z_{xy} \left(1 + \frac{\text{E noise power}}{\text{E signal power}}\right) \qquad (4.20)$$

and equation (4.19) gives

$$\bar{Z}_{xy} = \frac{\overline{E_{xs} H_{ys}^*}}{\overline{H_{ys} H_{ys}^*} + \overline{H_{yn} H_{yn}^*}} = Z_{xy} / \left(1 + \frac{\text{H noise power}}{\text{H signal power}}\right) \qquad (4.21)$$

Thus the estimate shown in equation (4.20) is biased to the high side by random noise on E while the one in equation (4.21) is biased to the low side by random noise on H. For similar percentages of random noise on E and H, an average of the various estimates hopefully will be better than any one estimate by itself. Also the scatter between the various estimates should be a good measure of the amount of random noise present.

In practice of course things are not quite this neat because the assumption that the cross terms in the average power estimates are negigible may not be valid. For example, terms of the form $\overline{E_{xn} H_{yn}^*}$ will not be

negligible if the two noises are coherent. Such might be the case for certain types of instrumentation noise or local industrial noise or 60 cps power line noise. Also terms of the form $\overline{E_{xs} E^*_{xn}}$ will not be negligible if the noise is coherent with the signal source. Even if all of the noise terms are random and independent of the signals and of each other, the cross terms may not be negligible if the average power estimates do not have enough degrees of freedom.

V. NOISE PROBLEMS

As was mentioned in the previous chapter, any physical measurement of E or H will include some noise. This noise may be in the form of a constant bias caused by inaccurate calibration of the measuring system, or it may be a nonlinear effect such as would result from drift in the sensitivity of the measuring system. On the other hand many types of noise are independent of the signal. These include such things as amplifier noise, 60 cps power line noise, digitizer round off noise, and, if the signals are recorded in analog form, tape recorder noise. Also, there is always the possibility of having source generated noise. For example, if the incident fields include some plane waves with horizontal wavelengths short compared to a skin depth in the earth, the resulting surface fields may be represented as containing noise.

In any event one can always represent the measured field components as sums of signals and noises as indicated in equations (4.14) through (4.17). The degree to which the noise terms are independent of the signal terms depends entirely upon the source of the noise. In the cases where the noise terms are dependent upon each other or upon the signal terms, the effects of the noise upon the Z estimates vary according to which estimates are used, and according to which signal and noise terms are coherent. No attempt has been made to catalogue all of the various possible combinations of signals and coherent noises.

For the situation where the noise terms are independent of each other and independent of the signals, some interesting results can be shown.

A. General Incoherent Noise

As was mentioned in the previous chapter, the various estimates of the elements of the Z matrix are biased either up by random noise on E or down by random noise on H. This is caused by the fact that the auto power

density spectra are in general biased up by random noise, while the cross power density spectra are not biased. For example, suppose that

$$E_x = E_{xs} + E_{xn} \tag{5.1}$$

and

$$H_y = H_{ys} + H_{yn} \tag{5.2}$$

where

$$\langle E_{xs} E^*_{xn} \rangle = 0 \tag{5.3}$$

$$\langle H_{ys} H^*_{yn} \rangle = 0 \tag{5.4}$$

$$\langle E_{xn} H^*_{yn} \rangle = 0 \tag{5.5}$$

and where the brackets < > denote "expected value of." Clearly, for this situation

$$\langle E_x E^*_x \rangle = \langle E_{xs} E^*_{xs} \rangle + \langle E_{xn} E^*_{xn} \rangle \tag{5.6}$$

$$\langle H_y H^*_y \rangle = \langle H_{ys} H^*_{ys} \rangle + \langle H_{yn} H^*_{yn} \rangle \tag{5.7}$$

and

$$\langle E_x H^*_y \rangle = \langle E_{xs} H^*_{ys} \rangle \tag{5.8}$$

Equation (5.8) implies that the cross power can be estimated to any arbitrary degree of accuracy by measuring the fields for a long enough period of time. On the other hand, equations (5.6) and (5.7) imply that the estimates of the auto powers will be biased regardless of the length of time that the fields are measured.

These ideas lead one to consider an alternate approach to the problem. Suppose that one performs two simultaneous independent measurements of one of the field components, say E_x. If the results are

$$E_{x1} = E_{xs} + E_{xn1} \tag{5.9}$$

and

$$E_{x2} = E_{xs} + E_{xn2} \tag{5.10}$$

where

$$\langle E_{xs} E^*_{xn1} \rangle = 0 \tag{5.11}$$

$$\langle E_{xs} E^*_{xn2} \rangle = 0 \tag{5.12}$$

and

$$\langle E_{xn1} E^*_{xn2} \rangle = 0 \tag{5.13}$$

then

$$\langle E_{x1} E^*_{x2} \rangle = \langle E_{xs} E^*_{xs} \rangle \tag{5.14}$$

Equation (5.14) implies that the E_x auto power density spectrum can be estimated to any arbitrary degree of accuracy from two simultaneous noisy measurements of E_x if the measurements are taken for a long enough period of time and if the noises on the two measurements are independent.

In general, if one has double measurements of either the two tangential components of E or the two tangential components of H, one can obtain estimates of the four elements of the Z matrix that are not biased by random noise.

B. Numerical Noise

At this time consideration will be given to several specific types of numerical noise. The term numerical noise as used here refers to any noise that is artificially injected into the signal when the latter is sampled for numerical processing.

1. Perhaps the most commonly recognized form of numerical noise is that which is usually referred to as aliasing. In accordance with the sampling theorem, if a continuous function which is sampled at a rate f_o has any frequency components greater than the Nyquist or folding frequency (equal to $f_o/2$), these components will be lost from the sampled version of the function.

If any spectral analysis is performed on the sampled function, the lost frequency components will appear folded down into the desired spectrum, and will of course represent noise. Since aliasing is a well documented and well understood phenomenon, nothing more will be said about it here except to note that anyone who deals with magnetotelluric data or any other form of sampled data should be aware of it.

2. The next type of noise that will be considered here is round off error on the analog-to-digital converter. This type of noise arises from the fact that the A-D converter has only a finite number of discrete levels. Typically the signal passes through many levels between sample points. For this reason, the noise can be characterized quite well as a sequence of independent random variables with amplitudes ranging from $\epsilon/2$ to $-\epsilon/2$ with a flat distribution where ϵ is the distance between adjacent levels on the A-D converter. Thus the noise spectrum will be flat. The total noise power for 2m data points will be

$$\text{Total Noise Power} = \frac{1}{\epsilon} \int_{-\epsilon/2}^{\epsilon/2} x^2 dx = \epsilon^2/12 \qquad (5.15)$$

Since the spectrum is flat, the average noise power per harmonic would be $\epsilon^2/12m$ for m harmonics. If the signal spectrum were also flat, the average signal power associated with each harmonic would be about $(M\epsilon)^2/12m$ where M is the number of digitizer levels that corresponds to the maximum peak to peak amplitude of the signal. Thus, the signal to noise ratio would be on the order of M^2. In practice, it frequently happens that the signal spectrum is not flat. In this case the expected signal to noise level for a given harmonic is about

$$M^2 \frac{\text{Signal power in harmonic}}{\text{Average signal power per harmonic}}$$

$$= M^2 m \frac{\text{Signal power in harmonic}}{\text{Total signal power}} \qquad (5.16)$$

if there is a total of m harmonics.

As an experimental check of the digitizer noise, the following was done. A typical set of actual magnetic field data was selected. It was Fourier transformed, and each harmonic was multiplied by a theoretical Z computed from a typical layered model.. The resulting theoretical E was Fourier transformed back to the time domain and digitized; that is, rounded off to a given number of significant bits. The resulting E together with the original H were used to compute an apparent resistivity versus frequency curve. Figure 7 shows the individual harmonics of the true E power density spectrum along with the expected digitizer noise levels for eight and twelve bit digitizing. Figures 8 and 9 show apparent resistivity versus frequency for the individual harmonics for eight and twelve bit digitizing together with the true ρ_a computed from the assumed model. Figures 10 through 12 give the corresponding results when the power density spectra are first averaged in bands of constant Q. From these figures, it is seen that, as expected, the apparent resistivities computed from the individual harmonics have random scatter when the signal power is not sufficiently large compared to the noise. Also as expected, the apparent resistivities computed from the averaged power estimates are biased to the high side by random digitizer noise on E. These experimental results are consistent with the theoretical discussion of digitizer noise.

3. The next type of numerical noise that will be considered is that which results from truncating the time series to a finite length T. Suppose that one of the field components has an amplitude that is described by f(t) for all time. The Fourier transform $F(\omega)$ is then given by

$$F(\omega) = \int_{-\infty}^{\infty} f(t)\ e^{-j\omega t}\ dt \qquad (5.17)$$

It is then desired to approximate $F(\omega)$ by $\bar{F}(n\omega_o)$, a Fourier series representation

of f(t) over some time interval T. Thus

$$\bar{F}(n\omega_o) = \int_{-T/2}^{T/2} f(t)\, e^{-jn\omega_o t}\, dt;\ n = 0 \pm 1, \pm 2, \ldots \tag{5.18}$$

where $\omega_o = 2\pi/T$.

Notice that

$$\bar{F}(\omega) = \int_{-\infty}^{\infty} f(t)\, d(t)\, e^{-j\omega t}\, dt \tag{5.19}$$

where $d(t) = 1$ for $|t| < T/2$ and $d(t) = 0$ for $|t| > T/2$. Thus, from the convolution theorem

$$\bar{F}(n\omega_o) = \int_{-\infty}^{\infty} F(\omega)\, D(n\omega_o - \omega)\, d\omega \tag{5.20}$$

where

$$\begin{aligned} D(\omega) &= \int_{-\infty}^{\infty} d(t)\, e^{-j\omega t}\, dt \\ &= \int_{-T/2}^{T/2} e^{-j\omega t}\, dt \\ &= \frac{2\pi}{\omega_o}\, \frac{\sin(\pi\omega/\omega_o)}{(\pi\omega/\omega_o)} \end{aligned} \tag{5.21}$$

$D(\omega)$ is usually called the spectral window since the observed spectrum $\bar{F}(\omega)$ is equal to the true spectrum $F(\omega)$ convolved with $D(\omega)$.

The spectral window defined by equation (5.21) is actually not very desirable since the side lobes go off only as $1/\omega$. A better window, usually known as the Hanning window is obtained by letting

$$d(t) = \begin{cases} .5 + .5 \cos \omega_o t & ;\ |t| < T/2 \\ 0 & ;\ |t| > T/2 \end{cases} \tag{5.22}$$

Then

$$D(\omega) = \int_{-T/2}^{T/2} (.5 + .5 \cos \omega_o t)\ e^{-j\omega t}\ dt$$

$$= \frac{\omega_o^2 \sin(\pi\omega/\omega_o)}{\omega(\omega_o^2 - \omega^2)} \qquad (5.23)$$

The main lobe of this spectral window is twice as wide as the main lobe of the previous one; however, the side lobes go off as $1/\omega^3$. The two windows are compared in figure 13.

One could define windows that have even smaller side lobes; however, they would necessarily have wider main lobes, and as will be seen later, this is not desirable. The Hanning window seems to be an adequate compromise between main lobe width and side lobe height.

One is then faced with the fact that any physical estimate of the power density at a particular frequency ω is necessarily a weighted average of the true power density over a band of frequencies, the weighting function being the spectral window $D(\omega)$. If the impedance function that one is attempting to estimate does not change significantly over the bandwidth defined by $D(\omega)$, then the estimate will not be corrupted by the truncation effects. In practice, however, the impedance does change some so that there will be some truncation noise. The problem is particularly severe if the power density spectra have resonant peaks or other steep slopes. If one is attempting to estimate the power density near the bottom of a steep slope, the contributions from the side lobes of the spectral window may be significant compared to the contribution from the main lobe. This effectively broadens the bandwidth over which the impedance function must not change.

These considerations lead one to inquire into the spectral behavior of the E and H fields used in magnetotelluric surveying. One would hope that the general shape of the spectra of the incident E and H fields might be more

or less independent of time and space coordinates. If this were the case, then the measured total H field, which is close to twice the incident H field, would also be reasonably stationary with respect to time and space coordinates, and hence it could be prewhitened. On the other hand, the total E field is a strong function of the local conductivity structure and hence, although it would be stationary with respect to time, the shape of the spectrum would change from one location to the next as the conductivity structure changes. But still, the surface impedance Z is a well behaved function of frequency and as such one would expect that if the E signals were passed through the same filters as were designed to prewhiten the H signals, the resulting filtered E signals would have a reasonably well behaved spectrum. This, in general, turns out to be the case. Actually, as is indicated by equations (2.16) and (2.27), Z tends on the average to be proportional to the square root of frequency, so that an optimum filter for E would differ from the H filter by a factor of $1/\sqrt{\omega}$.

With these ideas in mind, a study was made of the spectra of some actual H field data recorded in central Texas. Figures 14 and 15 give composite plots of H_x and H_y power density spectra obtained from 104 different data samples recorded at five different sites in central Texas. This data was recorded by D. R. Word, and a magnetotelluric interpretation of the data is given by him (Word, 1969). From these figures it is apparent that at least for the locations and times involved here, the general shape of the H power density spectra is fairly well defined. However, there are some definite resonant peaks (for example, around .07 cps and around 2.5 cps) that appear in some of the spectra but are absent from others. These results are consistent with those obtained by other investigators (Hopkins, 1966), (Bleil, 1964). It is believed that if the analog H signals are prewhitened according to the general trends shown in figures 14 and 15, the Hanning window can be used without encountering any side lobe difficulties except perhaps immediately adjacent to the observed resonances.

In order to get an estimate of the effects of truncation upon the individual harmonics of the Fourier spectra, consider the following problem. Assume a one dimensional case with

$$E(\omega) = Z(\omega)\ H(\omega)\ .$$

Suppose that the H signal is prewhitened with a filter that has a response $F_H(\omega)$, and the the E signal is passed through a filter whose response is $F_E(\omega)$ which may or may not be the same as $F_H(\omega)$. Assume that the outputs of these filters are $H_o(\omega)$ and $E_o(\omega)$ respectively, so that

$$Z(\omega) = \frac{E(\omega)}{H(\omega)} = \frac{E_o(\omega)}{H_o(\omega)} \cdot \frac{F_H(\omega)}{F_E(\omega)} \tag{5.24}$$

Then define

$$G(\omega) = \frac{E_o(\omega)}{H_o(\omega)} = \frac{Z(\omega)\, F_E(\omega)}{F_H(\omega)} \tag{5.25}$$

Thus $G(\omega)$ is the ratio of the prewhitened electric and magnetic field signals and will be equal to $Z(\omega)$ if the two prewhitening filters are the same. If the prewhitened signals are then sampled and a Fourier series analysis is performed on each, the results will be

$$\overline{H}(n\omega_o) = \int_{-\infty}^{\infty} H_o(n\omega_o - \omega)\ D(\omega)\ d\omega \tag{5.26}$$

and

$$\begin{aligned} \overline{E}(n\omega_o) &= \int_{-\infty}^{\infty} E_o(n\omega_o - \omega)\ D(\omega)\ d\omega \\ &= \int_{-\infty}^{\infty} H_o(n\omega_o - \psi)\ G(n\omega_o - \omega)\ D(\omega)\ d\omega \end{aligned} \tag{5.27}$$

where $D(\omega)$ is again the spectral window used. If G were constant over the

width of the window, then one would have

$$\overline{E}(n\omega_o) = G(n\omega_o) \int_{-\infty}^{\infty} H_o(n\omega_o - \omega)\, D(\omega)\, d\omega$$

$$= G(n\omega_o)\, \overline{H}(n\omega_o) \qquad (5.28)$$

the desired result. In practice however, G usually varies some. Suppose that in the neighborhood of $n\omega_o$, G can be represented by the first two terms of a Taylor series expansion. Thus

$$G(\lambda) = G(n\omega_o) + (\lambda - n\omega_o)\, G'(n\omega_o) \qquad (5.29)$$

where

$$G'(\omega) = \frac{dG(\omega)}{d\omega} \qquad (5.30)$$

If one lets $\lambda = n\omega_o - \omega$, equation (5.29) gives

$$G(n\omega_o - \omega) = G(n\omega_o) - \omega G'(n\omega_o) \qquad (5.31)$$

Putting this into equation (5.27) gives

$$\overline{E}(n\omega_o) = \int_{-\infty}^{\infty} H_o(n\omega_o - \omega)\, [G(n\omega_o) - \omega G'(n\omega_o)]\, D(\omega)\, d\omega$$

$$= G(n\omega_o)\, \overline{H}(n\omega_o) - G'(n\omega_o) \int_{-\infty}^{\infty} H_o(n\omega_o - \omega)\, D(\omega)\, \omega d\omega \qquad (5.32)$$

If one then defines

$$\overline{G}(n\omega_o) = \overline{E}(n\omega_o) / \overline{H}(n\omega_o) \qquad (5.33)$$

and

$$\text{error} = [\overline{G}(n\omega_o) - G(n\omega_o)] / G(n\omega_o) \qquad (5.34)$$

then from equation (5.32)

$$\bar{G}(n\omega_o) = G(n\omega_o) - G'(n\omega_o) \frac{\int_{-\infty}^{\infty} H_o(n\omega_o - \omega)\, D(\omega)\, \omega d\omega}{\int_{-\infty}^{\infty} H_o(n\omega_o - \omega)\, D(\omega)\, d\omega} \tag{5.35}$$

and

$$\text{error} = -\frac{G'(n\omega_o)}{G(n\omega_o)} \frac{\int_{-\infty}^{\infty} H_o(n\omega_o - \omega)\, D(\omega)\, \omega d\omega}{\int_{-\infty}^{\infty} H_o(n\omega_o - \omega)\, D(\omega)\, d\omega} \tag{5.36}$$

Assume now that the integrals in equation (5.36) can be approximated by summations of the form

$$\overline{H(n\omega_o)} = \int_{-\infty}^{\infty} H_o(n\omega_o - \omega)\, D(\omega)\, d\omega$$

$$= \sum_{i=-m}^{m} H_{on,i} D_i \tag{5.37}$$

where

$$H_{on,i} = H_o(n\omega_o - i\Delta\omega) \tag{5.38}$$

and

$$\sum_{i=-m}^{m} D_i = 1 \tag{5.39}$$

Then

$$\bar{W}(n\omega_o) = \int_{-\infty}^{\infty} H_o(n\omega_o - \omega)\, D(\omega)\, \omega d\omega$$

$$= \sum_{i=-m}^{m} H_{on,i} D_i \frac{i\Omega}{m} \tag{5.40}$$

where Ω is the maximum value of ω contributing to the integral. That is, $\omega = \Omega$ corresponds to $i = m$.

Assume that for any fixed n, $H_{on,i}$ are a sequence of $2m+1$ independent complex random variables whose components have normal distributions and zero means. Also assume that the original H signal was prewhitened enough so that over any given band, the expected value of the power density is constant. That is,

$$<H_{on,i}H^*_{on,i}> = \sigma_n^2 \; ; \; i = 0, \pm 1, \pm 2, \ldots \pm m \tag{5.41}$$

Since $H_{on,i}$ are assumed to be independent and have zero means,

$$<H_{on,i}> = 0 \tag{5.42}$$

and

$$<H_{on,i}H^*_{on,j}> = 0 \; ; \; i \neq j \tag{5.43}$$

Since $H_{on,i}$ are complex normal random variables, $\overline{H}(n\omega_o)$ and $\overline{W}(n\omega_o)$, which are linear combinations of $H_{on,i}$, must also be complex normal random variables. Consider the statistics of $\overline{H}(n\omega_o)$ and $\overline{W}(n\omega_o)$.

$$<\overline{H}(n\omega_o)> = <\sum_{i=-m}^{m} H_{on,i}D_i>$$

$$= \sum_{i=-m}^{m} <H_{on,i}> D_i$$

$$= 0 \tag{5.44}$$

$$<\overline{H}(n\omega_o)\overline{H}^*(n\omega_o)> = <\left(\sum_{i=-m}^{m} H_{on,i}D_i\right)\left(\sum_{j=-m}^{m} H^*_{on,j}D_j\right)>$$

(Eq. cont'd on next page)

$$= \sum_{i=-m}^{m} \sum_{j=-m}^{m} D_i D_j \langle H_{on,i} H^*_{on,j} \rangle$$

$$= \sum_{i=-m}^{m} D_i^2 \langle H_{on,i} H^*_{on,i} \rangle$$

$$= \sigma_n^2 \sum_{i=-m}^{m} D_i^2 \qquad (5.45)$$

$$\langle \overline{W}(n\omega_o) \rangle = \langle \sum_{i=-m}^{m} H_{on,i} D_i \frac{i\Omega}{m} \rangle$$

$$= \frac{\Omega}{m} \sum_{i=-m}^{m} \langle H_{on,i} \rangle D_i \, i$$

$$= 0 \qquad (5.46)$$

$$\langle \overline{W}(n\omega_o) \overline{W}^*(n\omega_o) \rangle = \langle \left(\sum_{i=-m}^{m} H_{on,i} D_i \frac{i\Omega}{m} \right) \left(\sum_{j=-m}^{m} H^*_{on,j} D_j \frac{j\Omega}{m} \right) \rangle$$

$$= \left(\frac{\Omega}{m} \right)^2 \sum_{i=-m}^{m} \sum_{j=-m}^{m} D_i D_j \, ij \langle H_{on,i} H^*_{on,j} \rangle$$

$$= \left(\frac{\Omega}{m} \right)^2 \sigma_n^2 \sum_{i=-m}^{m} i^2 D_i^2 \qquad (5.47)$$

$$\langle \overline{H}(n\omega_o) \overline{W}^*(n\omega_o) \rangle = \langle \left(\sum_{i=-m}^{m} H_{on,i} D_i \right) \left(\sum_{j=-m}^{m} H^*_{on,j} D_j \frac{j\Omega}{m} \right) \rangle$$

(Eq. cont'd.)

$$= \frac{\Omega}{m} \sum_{i=-m}^{m} \sum_{j=-m}^{m} D_i D_j \langle H_{on,i} H^*_{on,j} \rangle$$

$$= \frac{\Omega}{m} \sigma_n^2 \sum_{i=-m}^{m} i D_i^2 \tag{5.48}$$

If the spectral window $D(\omega)$ is an even function of ω, then $D_i^2 = D_{-i}^2$ and

$$\sum_{i=-m}^{m} i D_i^2 = 0 \tag{5.49}$$

so that

$$\langle \bar{H}(n\omega_o) \bar{W}^*(n\omega_o) \rangle = 0 \tag{5.50}$$

Thus, $\bar{H}(n\omega_o)$ and $\bar{W}(n\omega_o)$ are independent complex normal random variables with zero means and with variances defined by equations (5.45) and (5.47).

A standard exercise in random variable theory indicates that if two random variables X and Y are normal and independent with zero means and equal variances, then the function

$$V = \sqrt{X^2 + Y^2}$$

has a Rayleigh distribution (see for example, Papoulis, 1965). Since $\bar{H}(n\omega_o)$ and $\bar{W}(n\omega_o)$ are complex normal random variables with zero means, their real and imaginary parts satisfy the conditions of the above exercise. Thus $|\bar{H}(n\omega_o)|$ and $|\bar{W}(n\omega_o)|$ must have Rayleigh distributions.

Another standard exercise in random variable theory indicates that if

$$V = X/Y$$

then the distribution of V is given by

$$F_V(v) = \int_0^{\infty} \int_{-\infty}^{yv} f_{XY}(x,y)\, dx\, dy + \int_{-\infty}^{0} \int_{yv}^{\infty} f_{XY}(x,y)\, dx\, dy \tag{5.51}$$

where $f_{XY}(x,y)$ is the joint density of X and Y (see Papoulis, 1965). If X and Y are independent and have Rayleigh distributions then equation (5.51) becomes

$$F_V(v) = \int_0^\infty \int_0^{yv} f_X(x)\, f_Y(y)\, dx\, dy$$

$$= \int_0^\infty f_Y(y)\, F_X(yv)\, dy$$

$$= \int_0^\infty \frac{y}{\alpha_y^2}\, e^{-y^2/2\alpha_y^2} \left[1 - e^{-(yv)^2/2\alpha_x^2}\right] dy$$

$$= 1 - \frac{1}{1 + \left(\frac{v\alpha_y}{\alpha_x}\right)^2} \qquad (5.52)$$

where $\alpha_x^2 = \langle X^2 \rangle$ and $\alpha_y^2 = \langle Y^2 \rangle$.

Now recall that $|\overline{H}(n\omega_o)|$ and $|\overline{W}(n\omega_o)|$ have Rayleigh distributions. From equations (5.45) and (5.47)

$$\langle |\overline{H}(n\omega_o)|^2 \rangle = \sigma_n^2 \sum_{i=-m}^{m} D_i^2 \qquad (5.53)$$

and

$$\langle |\overline{W}(n\omega_o)|^2 \rangle = \left(\frac{\Omega}{m}\right)^2 \sigma_n^2 \sum_{i=-m}^{m} i^2 D_i^2 \qquad (5.54)$$

Also, from equations (5.36), (5.37), and (5.40),

$$|\text{error}| = \left| \frac{G(n\omega_o)\, \overline{W}(n\omega_o)}{G'(n\omega_o)\, \overline{H}(n\omega_o)} \right| \qquad (5.55)$$

Recall that $F_V(v)$ is by definition the probability that $V \le v$. Thus, equations

(5.52) through (5.55) combine to give

$$P\{|\text{error}| \le \epsilon\} = 1 - \frac{1}{1 + (\epsilon \left| \frac{G(n\omega_o)}{G'(n\omega_o)} \right| K)^2} \tag{5.56}$$

where

$$K^2 = \frac{\sum_{i=-m}^{m} D_i^2}{(\frac{\Omega}{m})^2 \sum_{i=-m}^{m} i^2 D_i^2} \tag{5.57}$$

and where $P\{X\}$ denotes the probability, then X occurs. Recall from equations (5.37) through (5.40) that the summations arose as approximations to integrals. If one now lets $m \to \infty$ and passes back to the integral formulation, equation (5.57) becomes

$$K^2 = \frac{\int_{-\infty}^{\infty} D^2(\omega)\, d\omega}{\int_{-\infty}^{\infty} \omega^2 D^2(\omega)\, d\omega} \tag{5.58}$$

Since $D(\omega)$ has been assumed to be an even function of ω, and since

$$P\{|\text{error}| > \epsilon\} = 1 - P\{|\text{error}| \le \epsilon\}$$

one has from equation (5.56)

$$P\{|\text{error}| > \epsilon\} = \frac{1}{1 + \epsilon^2 \left| \frac{G(n\omega_o)}{G'(n\omega_o)} \right|^2 \frac{\int_0^{\infty} D(\omega)^2\, d\omega}{\int_0^{\infty} \omega^2 D(\omega)^2 d\omega}} \tag{5.59}$$

If $D(\omega)$ is a block window of width BW, equation (5.59) becomes

$$P\{|\text{error}| > \epsilon\} = \frac{1}{1 + \frac{12\epsilon^2}{(BW)^2}\left|\frac{G(n\omega_o)}{G'(n\omega_o)}\right|^2}$$

or

$$P\{|\text{error}| > \epsilon\} = \frac{1}{1 + 12\epsilon^2\left|\frac{G(n\omega_o)}{\Delta G(n\omega_o)}\right|^2} \tag{5.60}$$

where $\Delta G(n\omega_o) = G'(n\omega_o) \cdot BW$ = change in $G(\omega)$ over a band of width BW around $n\omega_o$. Similarly, for the Hanning window with

$$D(\omega) = \text{Sin}\,\frac{\pi\omega}{\omega_o}\left(\frac{\omega_o^2}{\omega(\omega_o^2 - \omega^2)}\right) \tag{5.61}$$

one obtains

$$P\{|\text{error}| > \epsilon\} = \frac{1}{1 + \frac{3\epsilon^2}{\omega_o^2}\left|\frac{G(n\omega_o)}{G'(n\omega_o)}\right|^2} \tag{5.62}$$

It has been observed that for one dimensional models

$$-\frac{1}{2} \leq \frac{d\log\sigma_a(\omega)}{d\log\omega} \leq \frac{1}{2} \tag{5.63}$$

Now if one uses the same prewhitening filters on E and H

$$|G(\omega)| = |Z(\omega)| = \sqrt{\omega\mu/\sigma_a(\omega)} \tag{5.64}$$

and it follows that

$$\frac{1}{4} \leq \frac{d\log|G(\omega)|}{d\log\omega} \leq \frac{3}{4} \tag{5.65}$$

or

$$\frac{d\log|G(\omega)|}{d\log\omega} = \frac{\omega}{|G(\omega)|}\frac{d|G(\omega)|}{d\omega} \leq \frac{3}{4} \tag{5.66}$$

or, for the worst case

$$\left| \frac{G(n\omega_o)}{G'(n\omega_o)} \right| \sim \frac{4n\omega_o}{3} \tag{5.67}$$

Thus, for this case equation (5.62) becomes

$$P\{|\text{error}| > \epsilon\} = \frac{1}{1 + \frac{16}{3} n^2 \epsilon^2} \tag{5.68}$$

Equation (5.68) indicates that, as expected, the probability of the error being greater than ϵ goes down as ϵ increases. Also, as expected, the probable error decreases as n, the harmonic number, increases. The latter result is expected since $|\Delta G(\omega)/G(\omega)|$ should be proportional to the percentage bandwidth of the window, which in turn is inversely proportional to the harmonic number. The results of equation (5.68) are summarized in figure 16.

It is doubtful that the results shown in figure 16 are useful quantitatively because of the assumptions made about the form of $H_o(\omega)$, the prewhitened magnetic field signal. In particular, it was assumed that $\sigma^2_{H_o} = \langle H_o(\omega) H_o(\omega)^* \rangle$ is independent of frequency. In practice this is not attainable since, as noted earlier, magnetotelluric signals are not really stationary.

In order to get some type of estimate of the effects of truncation upon realistic data, the following experiment was performed. A typical set of actual magnetic field data was selected. It was Fourier transformed using the Hanning window, and each harmonic was multiplied by a theoretical Z computed from a typical layered model. The resulting theoretical E was Fourier transformed back to the time domain. This E, together with the original H, were truncated to some fraction of the original length. The resulting truncated E and H signals were Fourier transformed, and apparent resistivities were computed from each harmonic. These apparent resistivities were then compared with the true apparent resistivities for the assumed model. This experiment

was repeated for several different models with several different original data lengths and several different truncated data lengths. The results showed a very definite trend. In each case, the apparent resistivities computed from the first eight to ten harmonics were significantly in error. The higher harmonics showed very little error. The amount of error on the first few harmonics depended significantly upon how white the spectra were; the whiter spectra had less error. Figures 17 and 18 show the results of a typical run. Figure 17 shows the individual harmonics of the spectrum of a truncated H signal. Figure 18 shows the corresponding apparent resistivities along with the true apparent resistivity curve for the assumed model.

These considerations lead one to believe that the first few harmonics of a Fourier spectrum of typical magnetotelluric data are likely to be corrupted considerably by truncation error.

VI. CONCLUSION

The methods of analysis discussed in the foregoing chapters have been implemented in a digital computer program constructed by the author for use on the CDC 6600 computer at The University of Texas Computation Center. This program estimates the power density spectra of sampled E and H signals by computing the Fourier transforms of the sampled data using the Cooley-Tukey algorithm, and averaging the resulting auto and cross powers in frequency bands of constant percentage bandwidth as discussed in Chapter IV, Section B.4. The Hanning window discussed in Chapter V, Section B.3 is used for the Fourier transforms. The elements of the Z matrix are then estimated from the power density spectra using the techniques described in Chapter IV, Section C. The principal axes are then determined in accordance with the discussion in Chapter III, Sections C and D. Also the approximate strike direction is determined from the vertical magnetic field as discussed in Chapter III, Section E. As diagnostics, the tensor coherency mentioned in Chapter IV, Section C, and the two-dimensionality parameters mentioned in Chapter III, Section D, are determined.

This program has been used extensively for analysis of magnetotelluric data recorded in central Texas by Darrell Word. Samples of the results are given by Word (1969). For most of the data analyzed using this program, the resulting surface impedance estimates have been consistent and repeatable. In areas where the geology is reasonably one dimensional, these surface impedances have been successfully interpreted in terms of horizontally layered models. The resulting resistivity profiles have agreed quite well with independent observations such as resistivity well logs in cases where the latter have been available.

In areas where the geology is more complex, particularly where it is highly three dimensional, interpretation has not been so successful. However, even here the surface impedance estimates have been fairly repeatable. Thus,

it is believed that now, perhaps for the first time, the surface impedances have been measured more accurately than they can at present be interpreted. For this reason, it is believed that future contributions to the science of magnetotellurics must come in the area of interpretation.

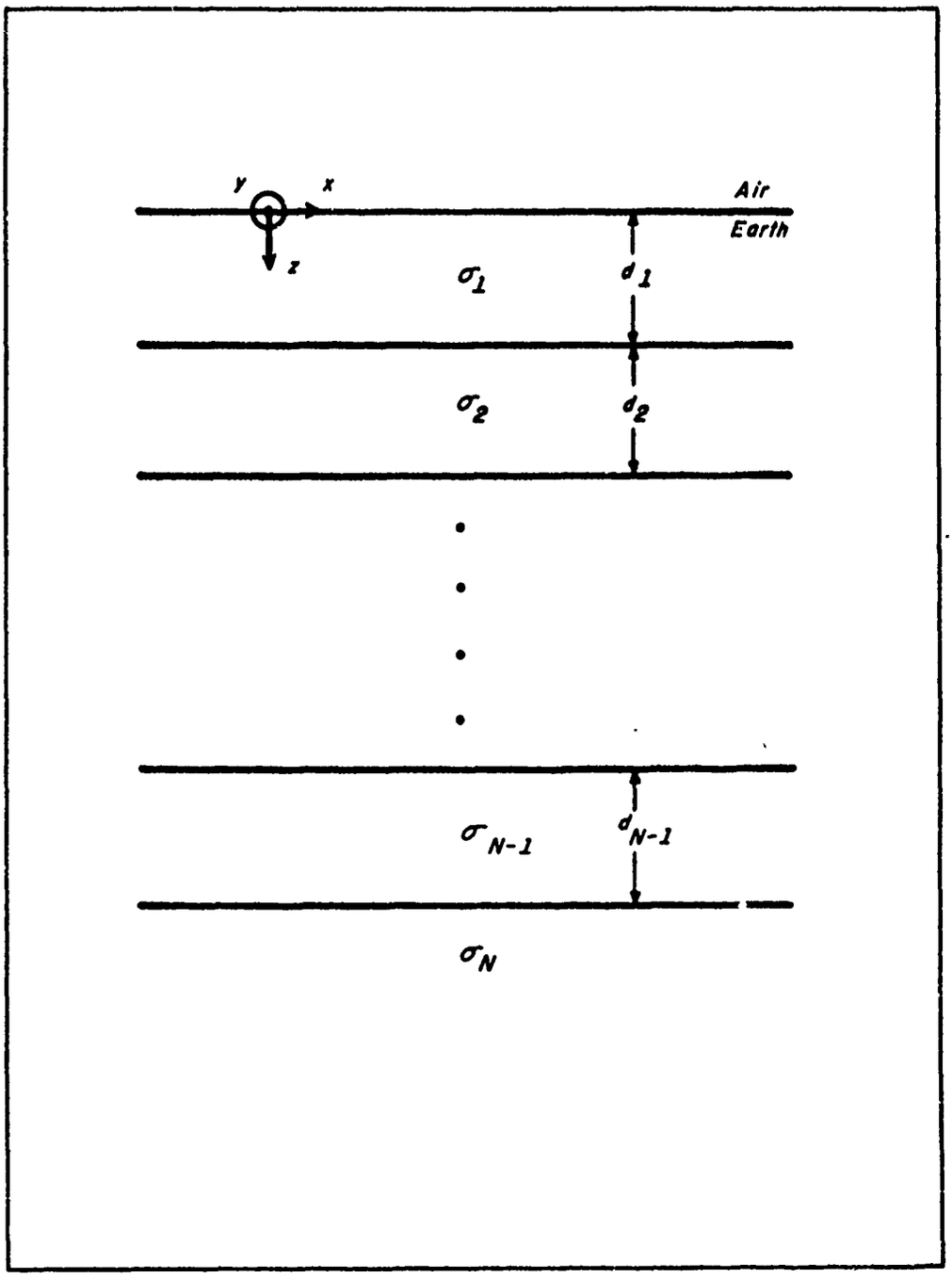

Fig. 1 Description of N Layer Model

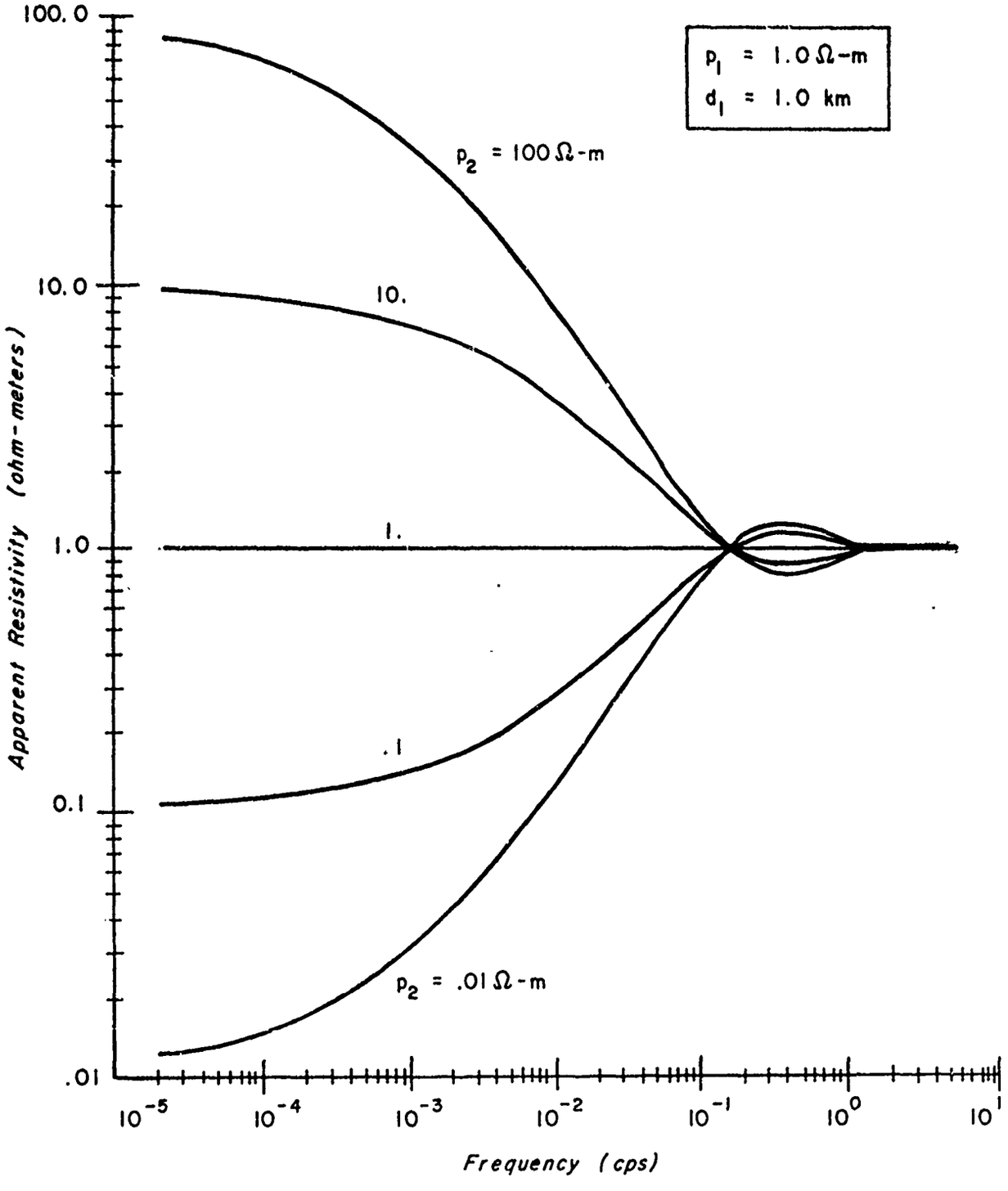

Fig. 2 Sample Two Layer Apparent Resistivity Curves

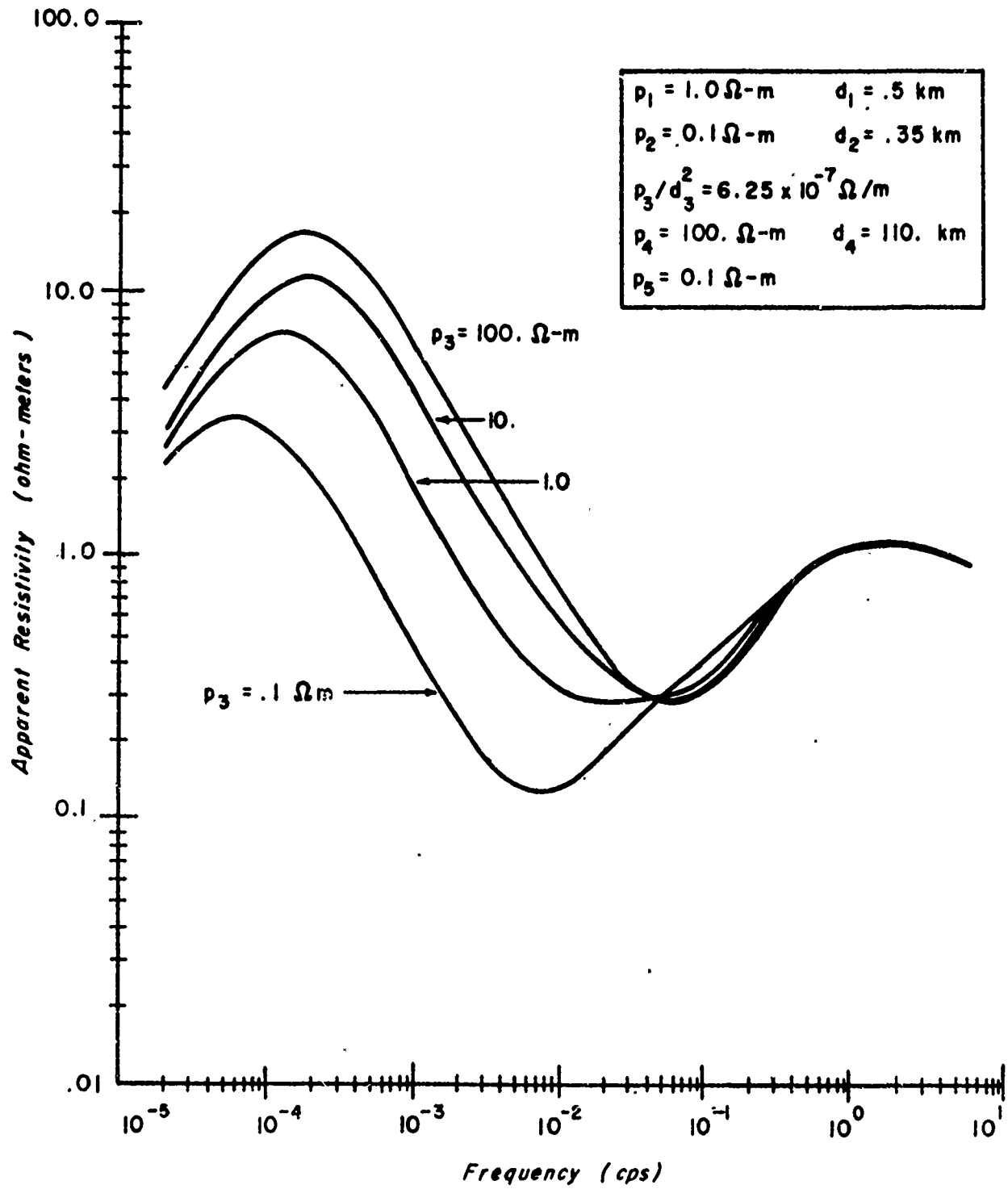

Fig. 3 Sample Five Layer Apparent Resistivity Curves

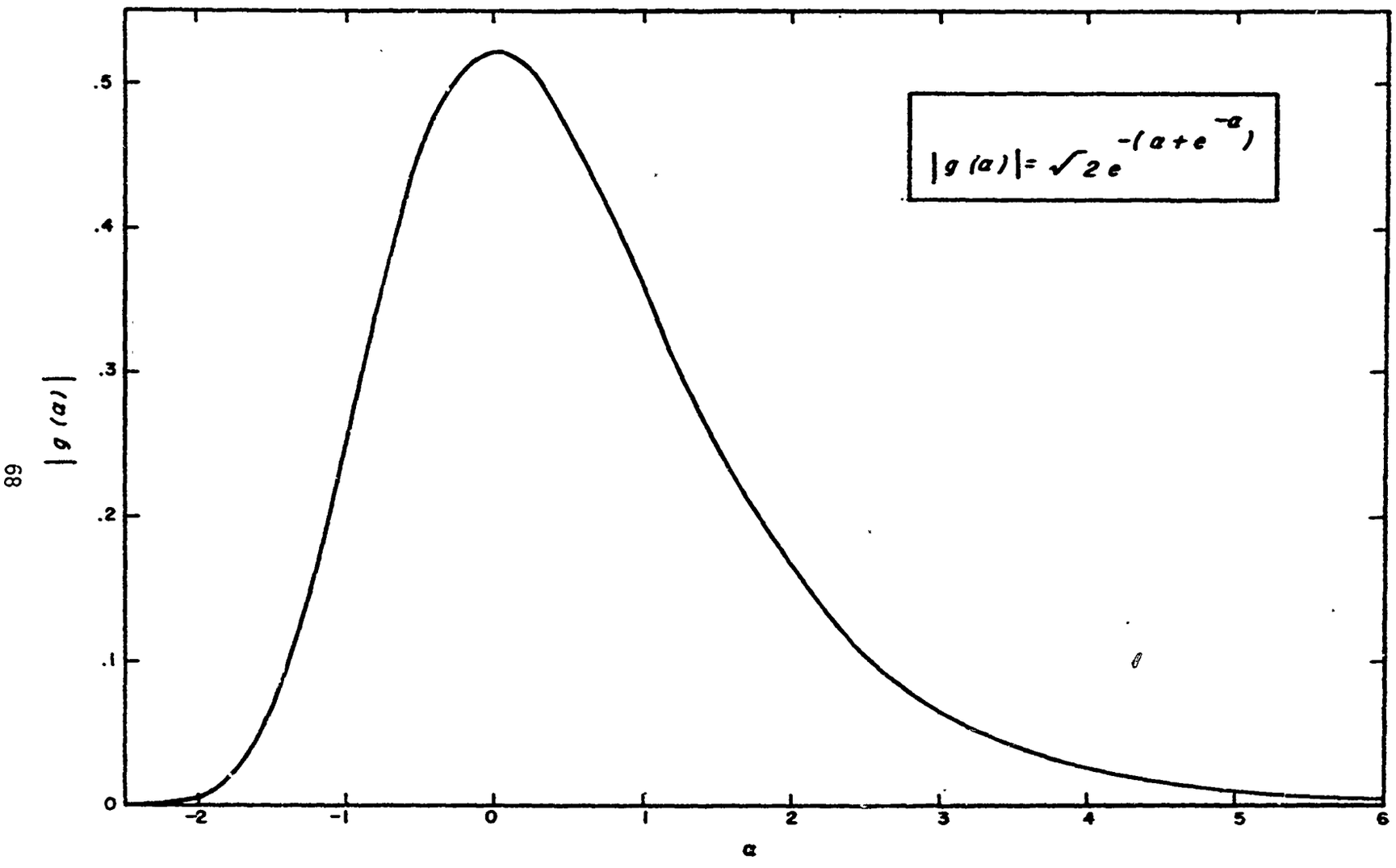

Fig. 4 Convolver for Linearized One Dimensional Problem

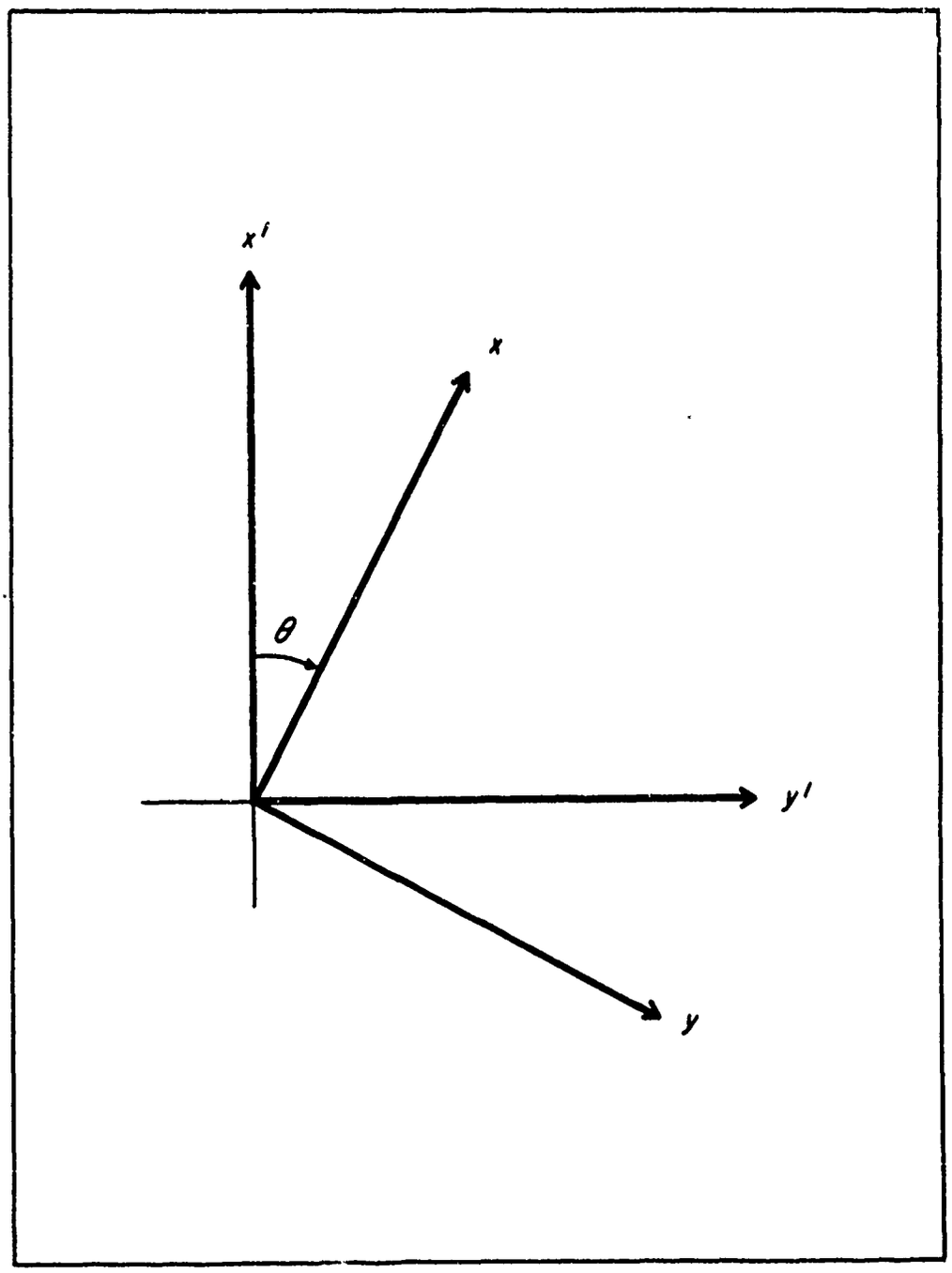

Fig. 5 Relative Orientation of x'-y' and x-y Coordinate Systems

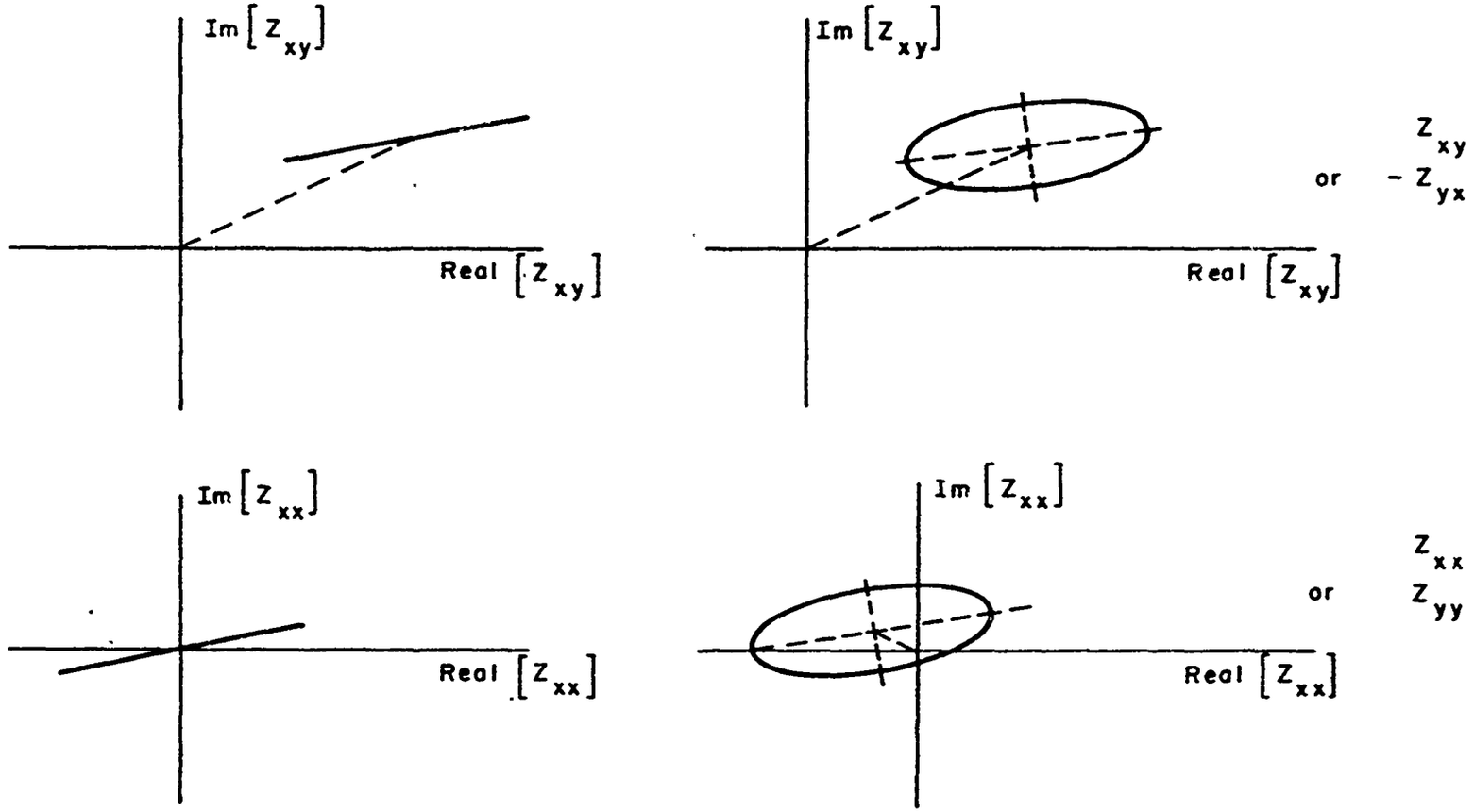

Fig. 6 Locii of Z_{ij} in the Complex Plane as the Measuring Axes are Rotated

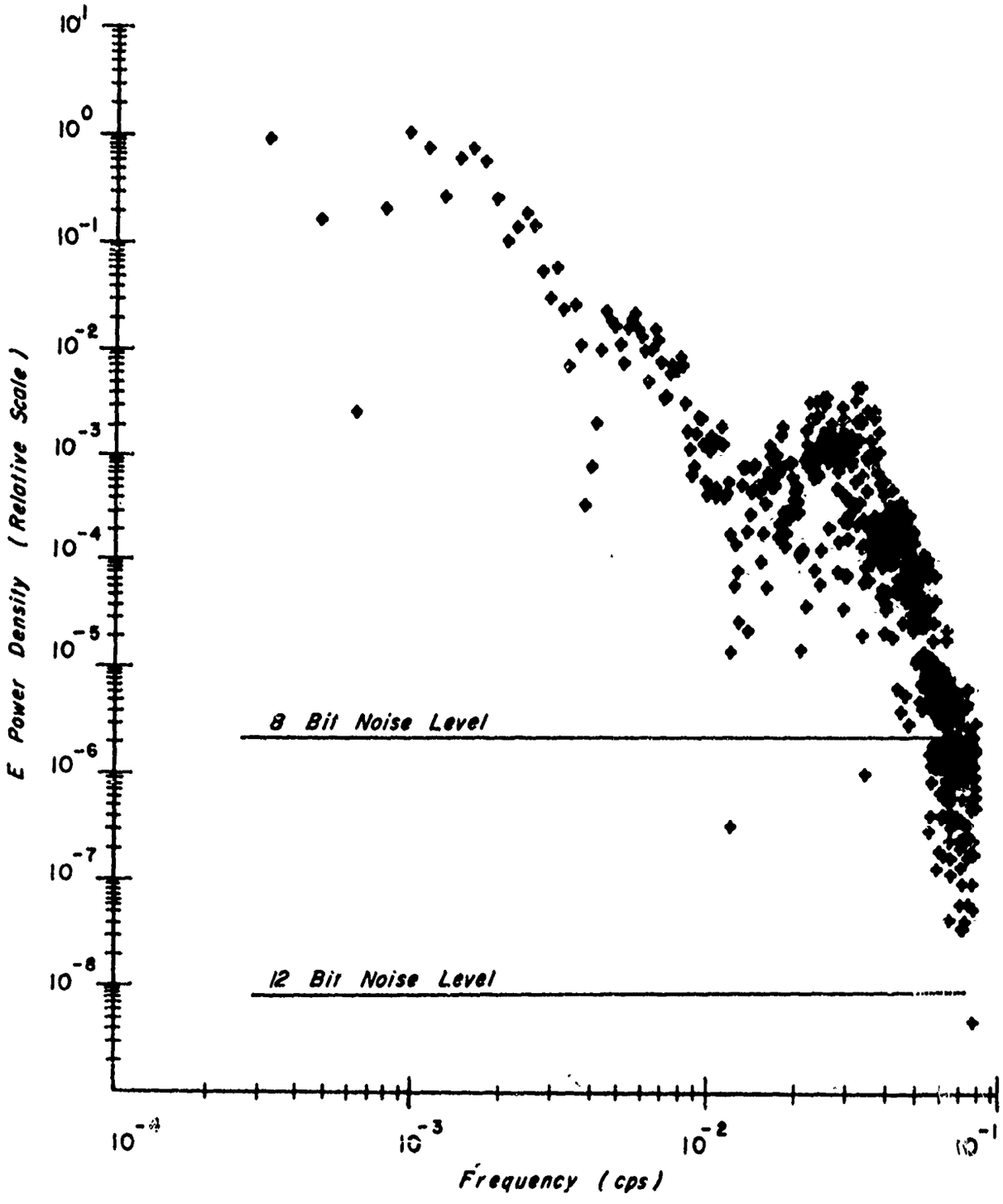

Fig. 7 Individual Harmonics of E Power Density Spectrum for Digitizer Noise Test with Expected Noise Levels for Eight and Twelve Bit Digitizing

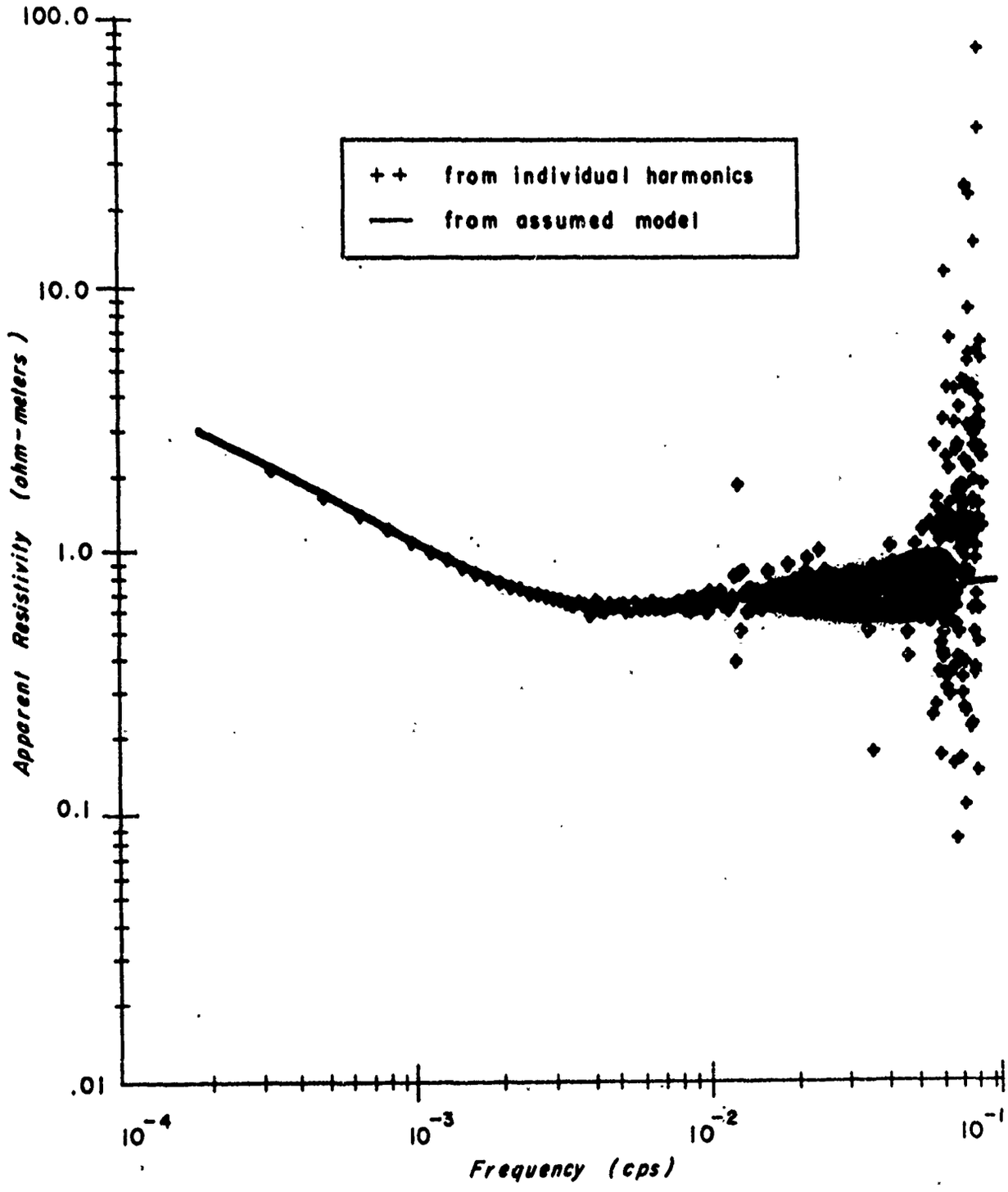

Fig. 8 Apparent Resistivity versus Frequency for Individual Harmonics for Eight Bit Digitizing

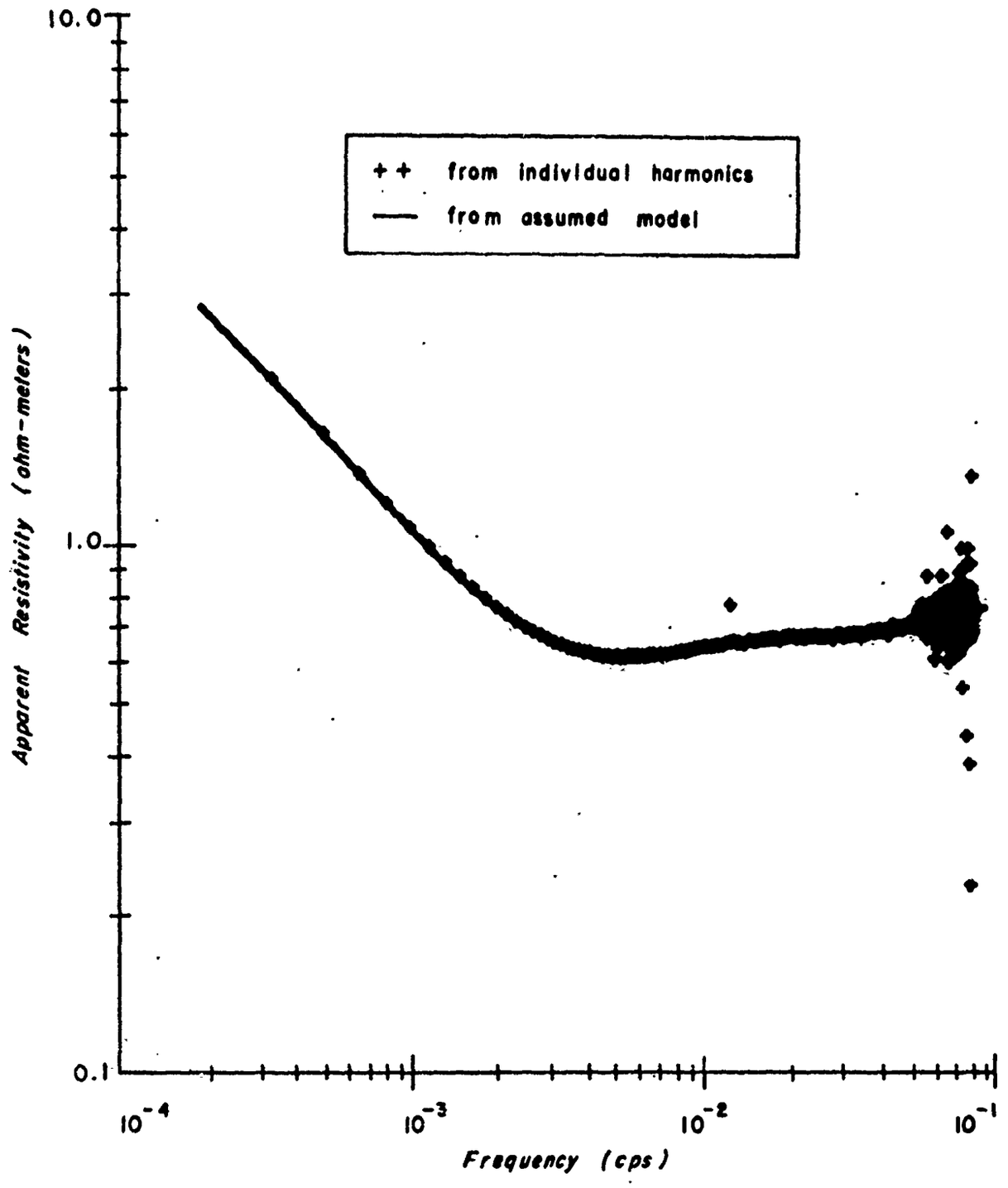

Fig. 9 Apparent Resistivity versus Frequency for Individual Harmonics for Twelve Bit Digitizing

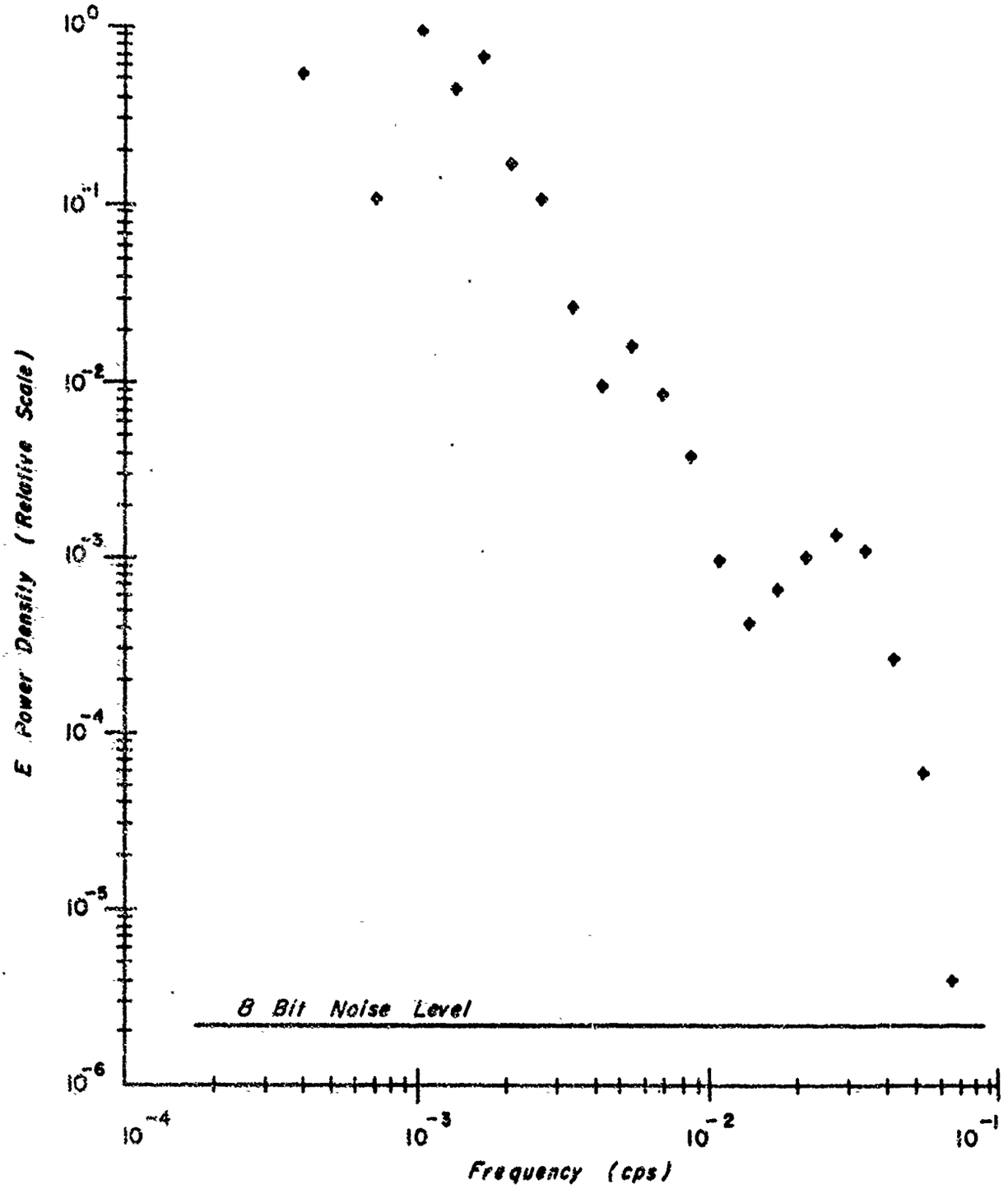

Fig. 10 Average E Power Density Spectrum for Digitizer Noise Test with Expected Noise Level for Eight Bit Digitizing

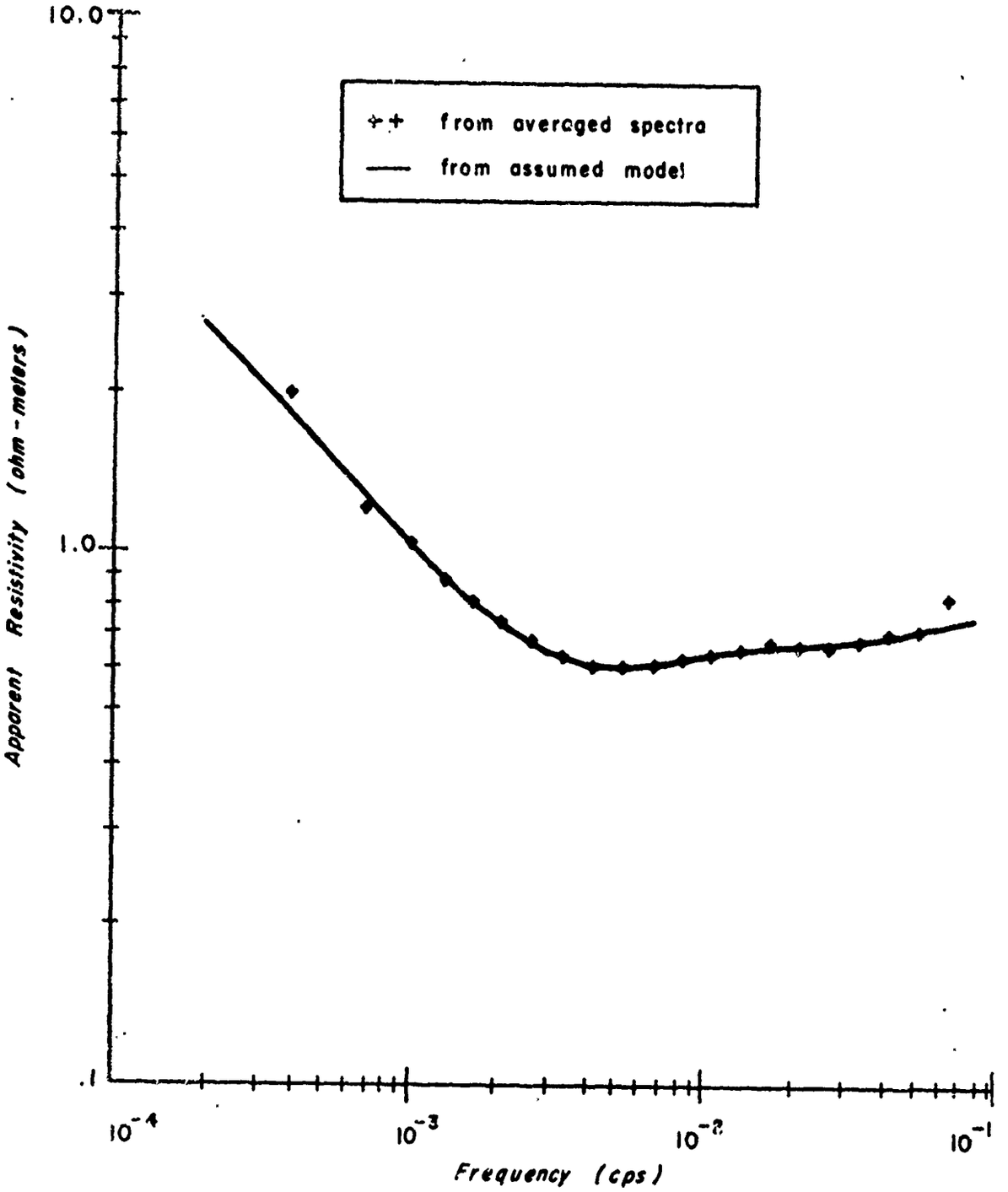

Fig. 11 Apparent Resistivity versus Frequency for Average Power Density Spectra with Eight Bit Digitizing

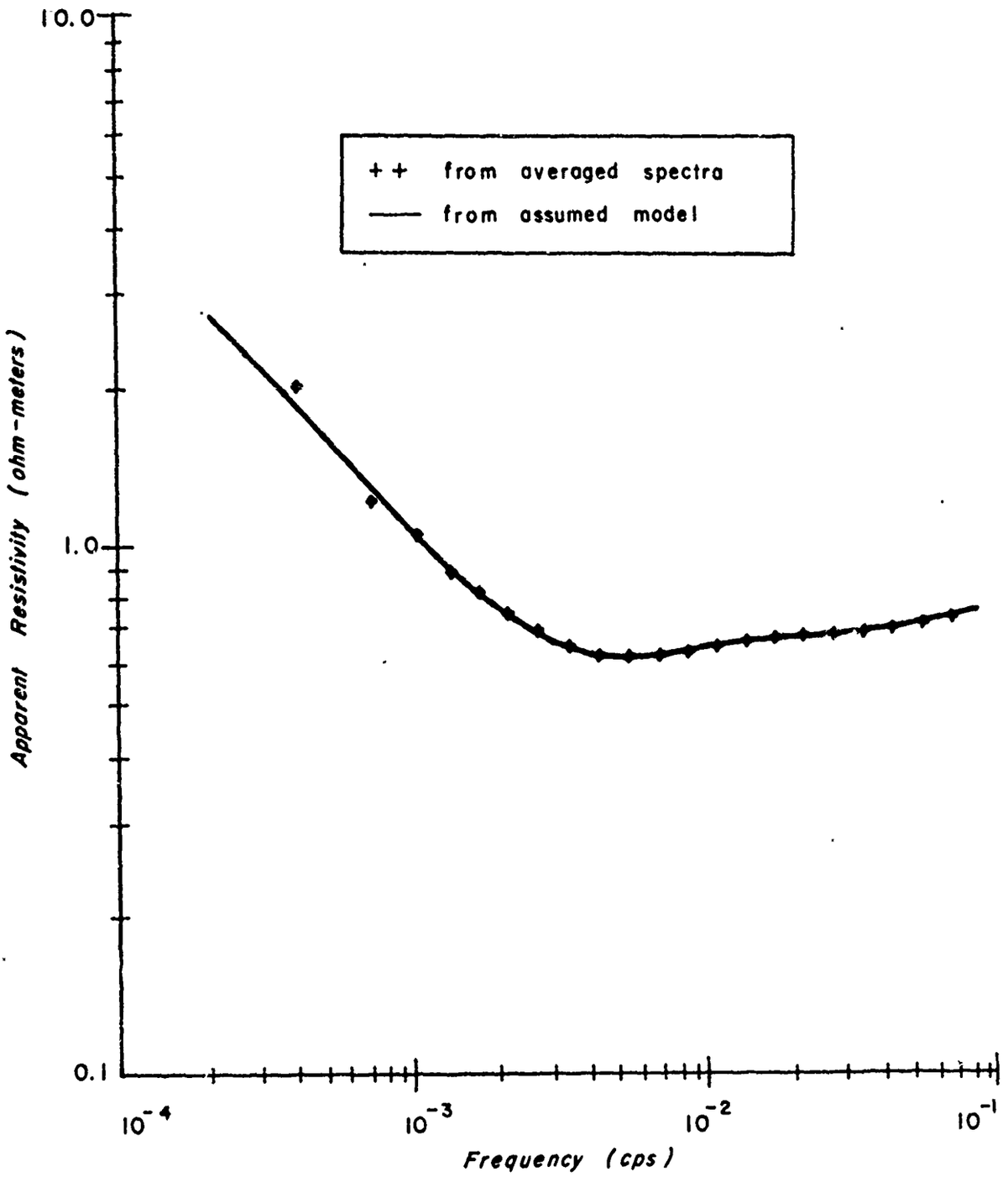

Fig. 12 Apparent Resistivity versus Frequency for Average Power Density Spectra with Twelve Bit Digitizing

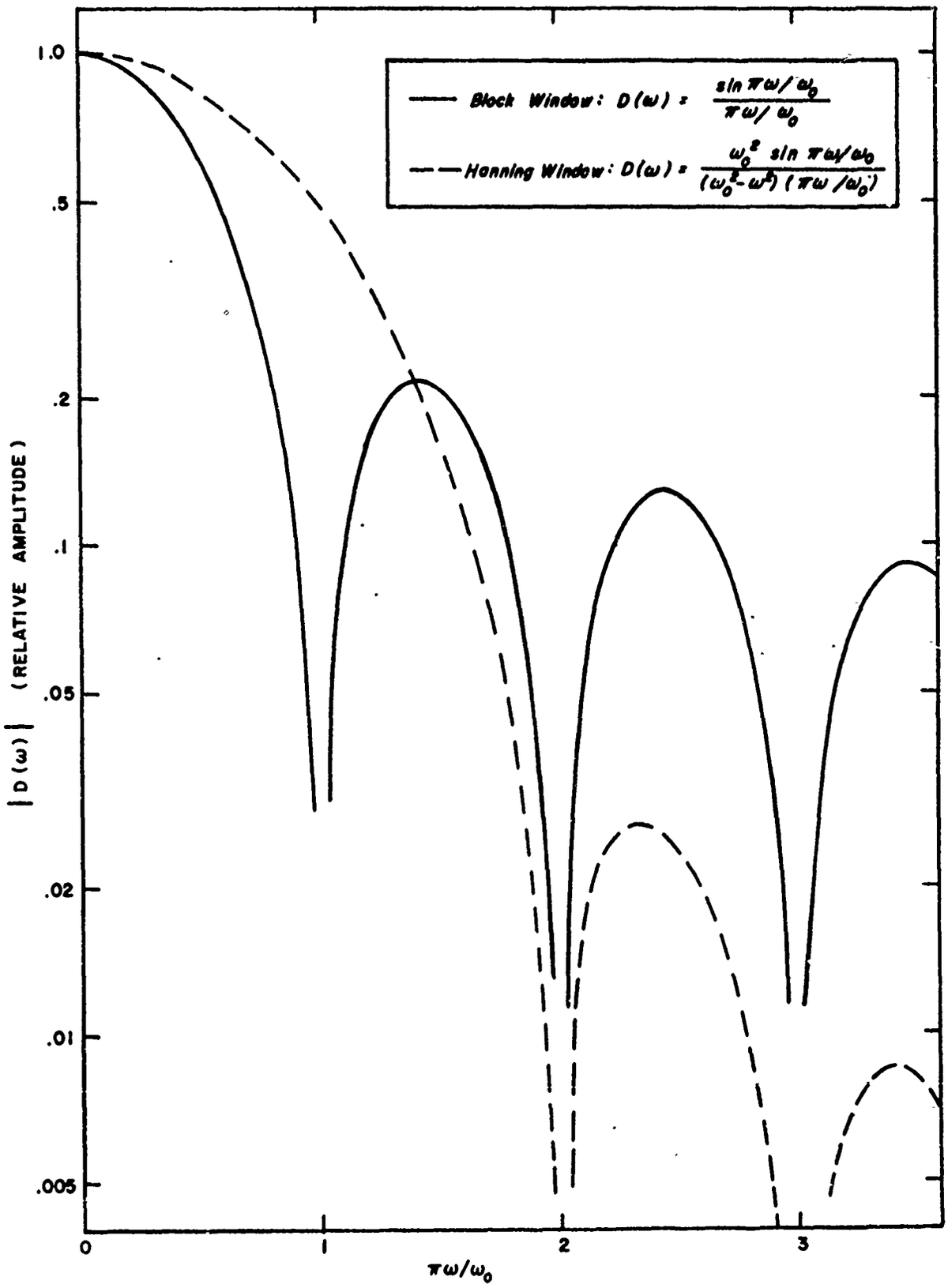

Fig. 13 Comparison of the Block and Hanning Spectral Windows

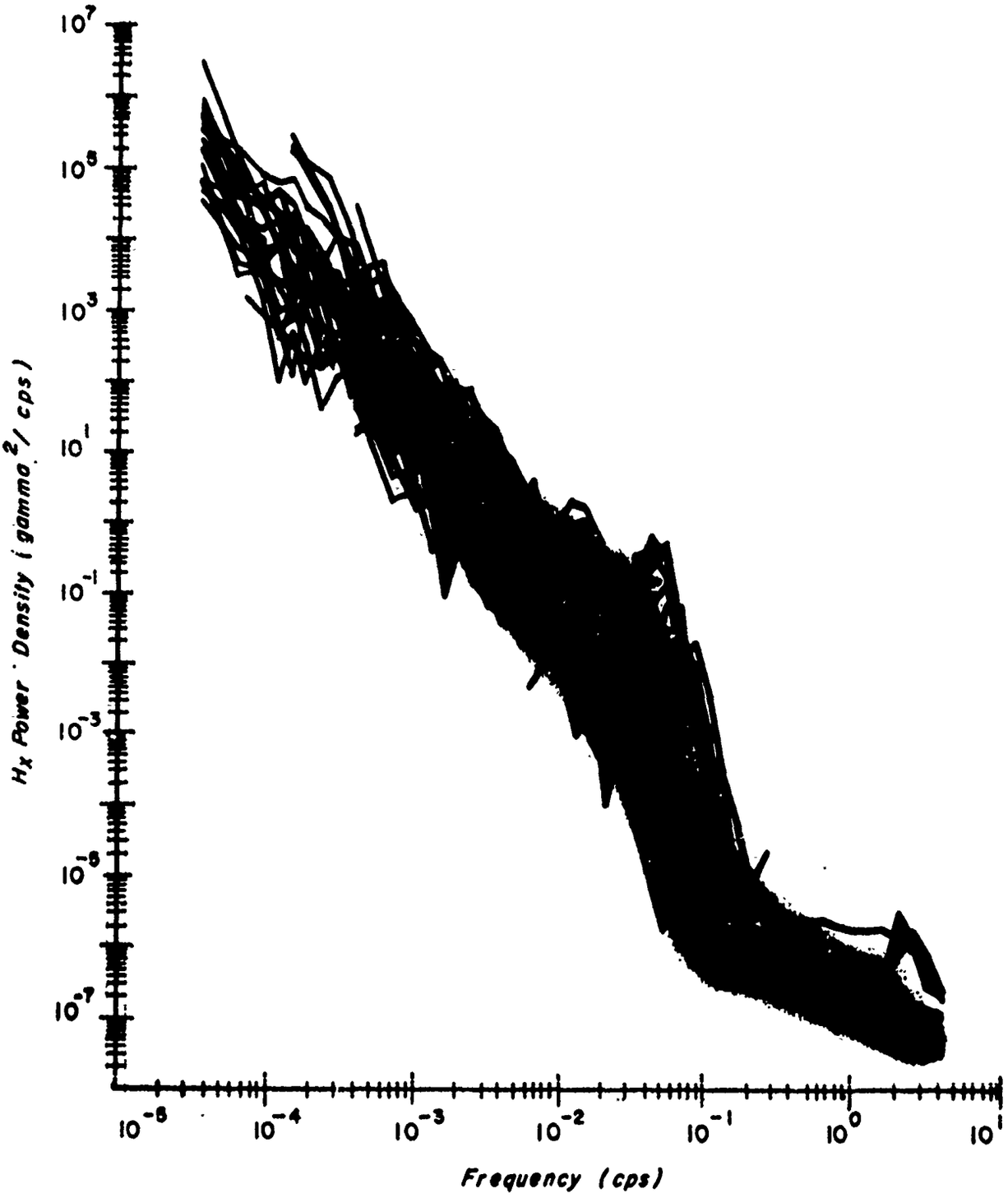

Fig. 14 H_x Power Density Spectra for 104 Different Data Samples Recorded in Central Texas

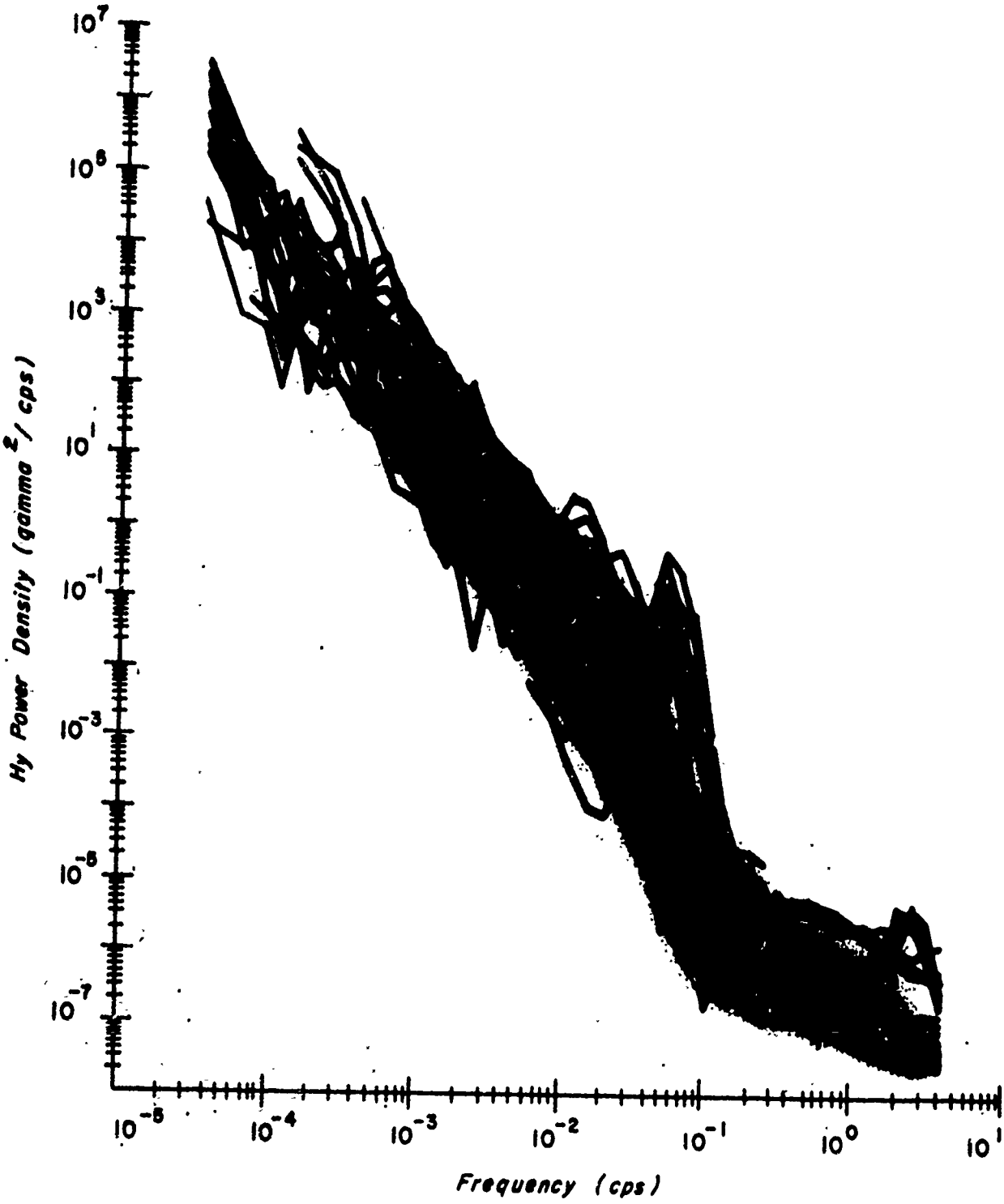

Fig. 15 H_y Power Density Spectra for 104 Different Data Samples Recorded in Central Texas

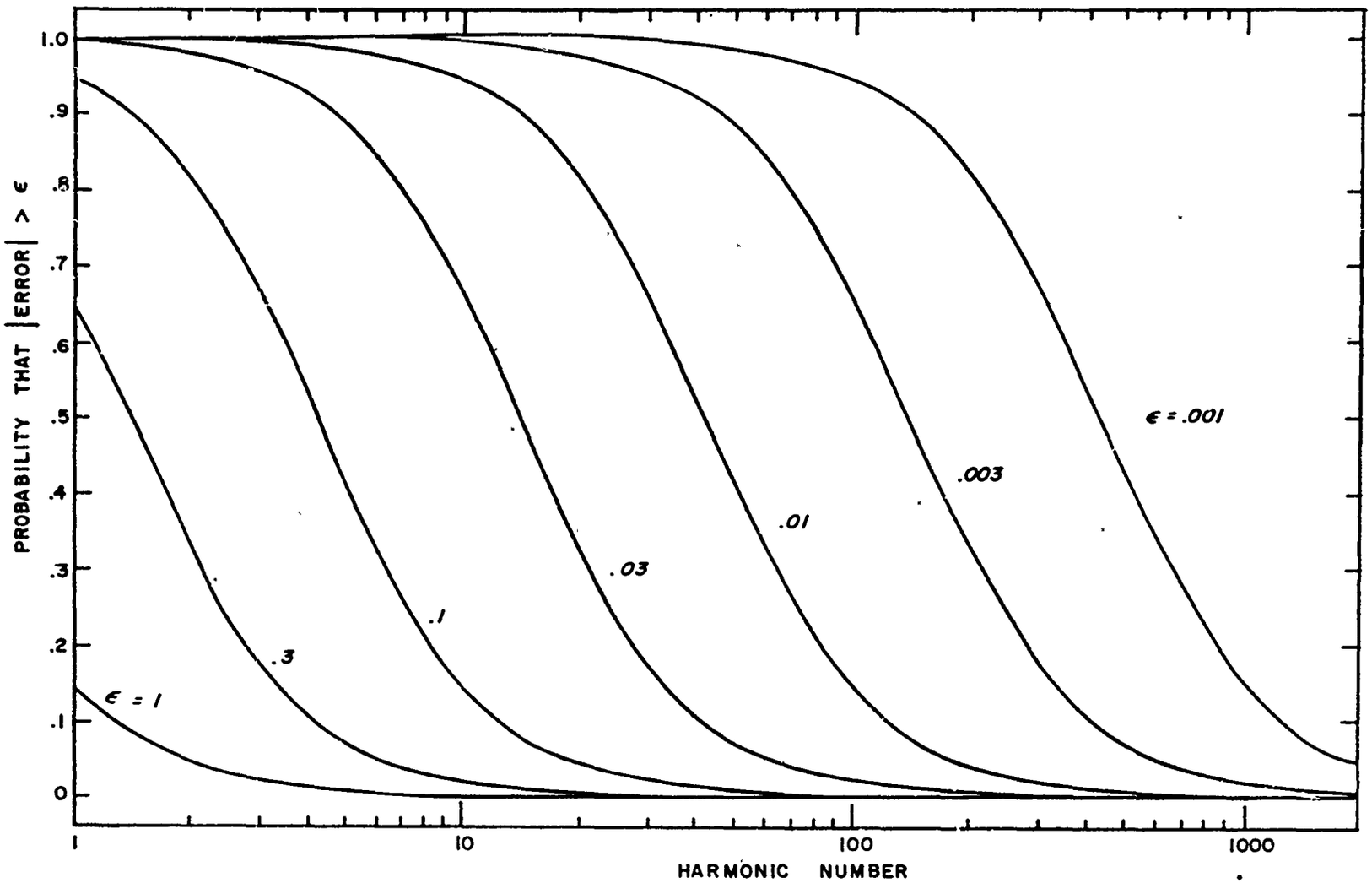

Fig. 16 Probability of Truncation Error on Impedance Estimates from Individual Harmonics

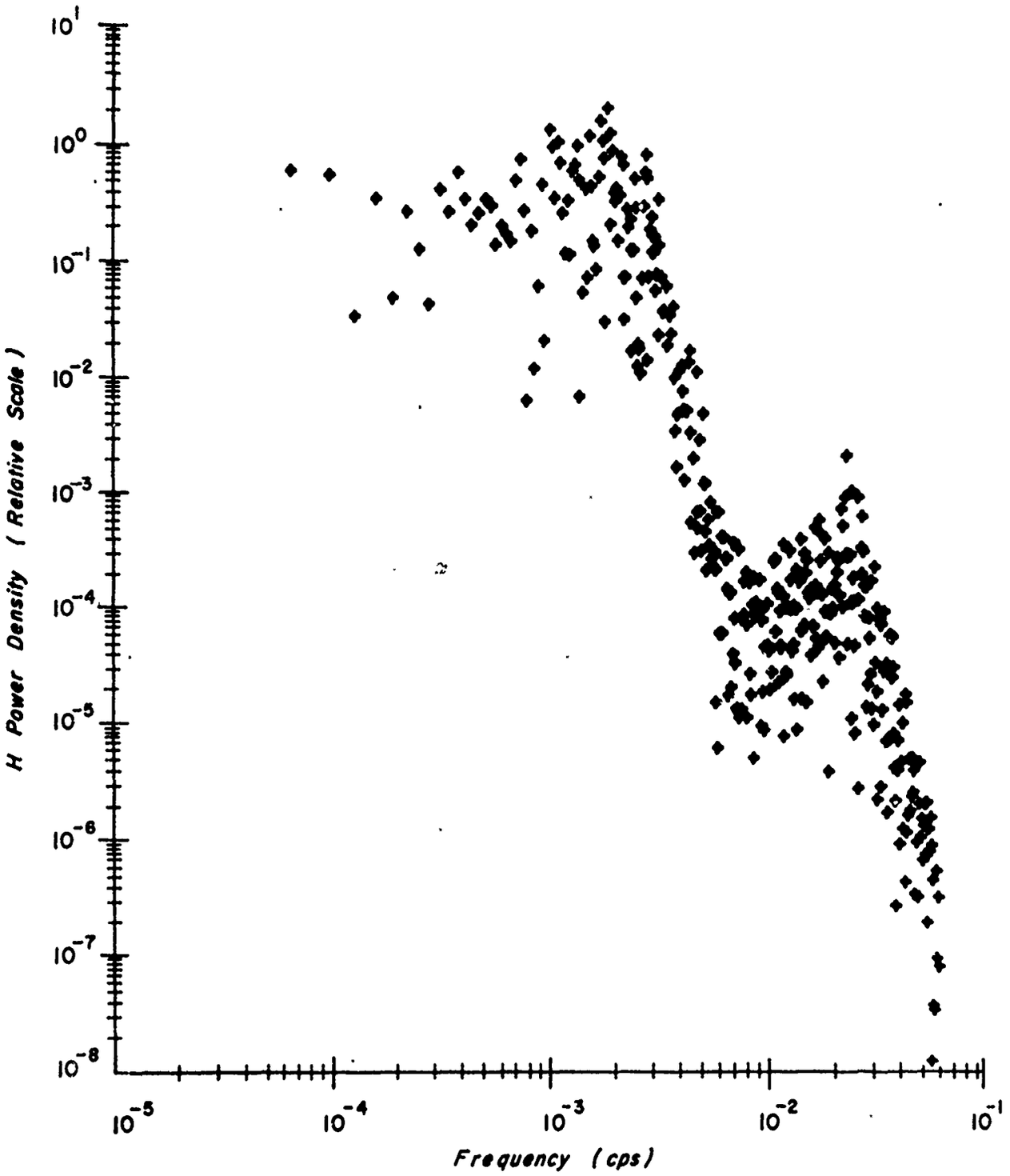

Fig. 17 Individual Harmonics of the Spectrum of a Truncated H Signal

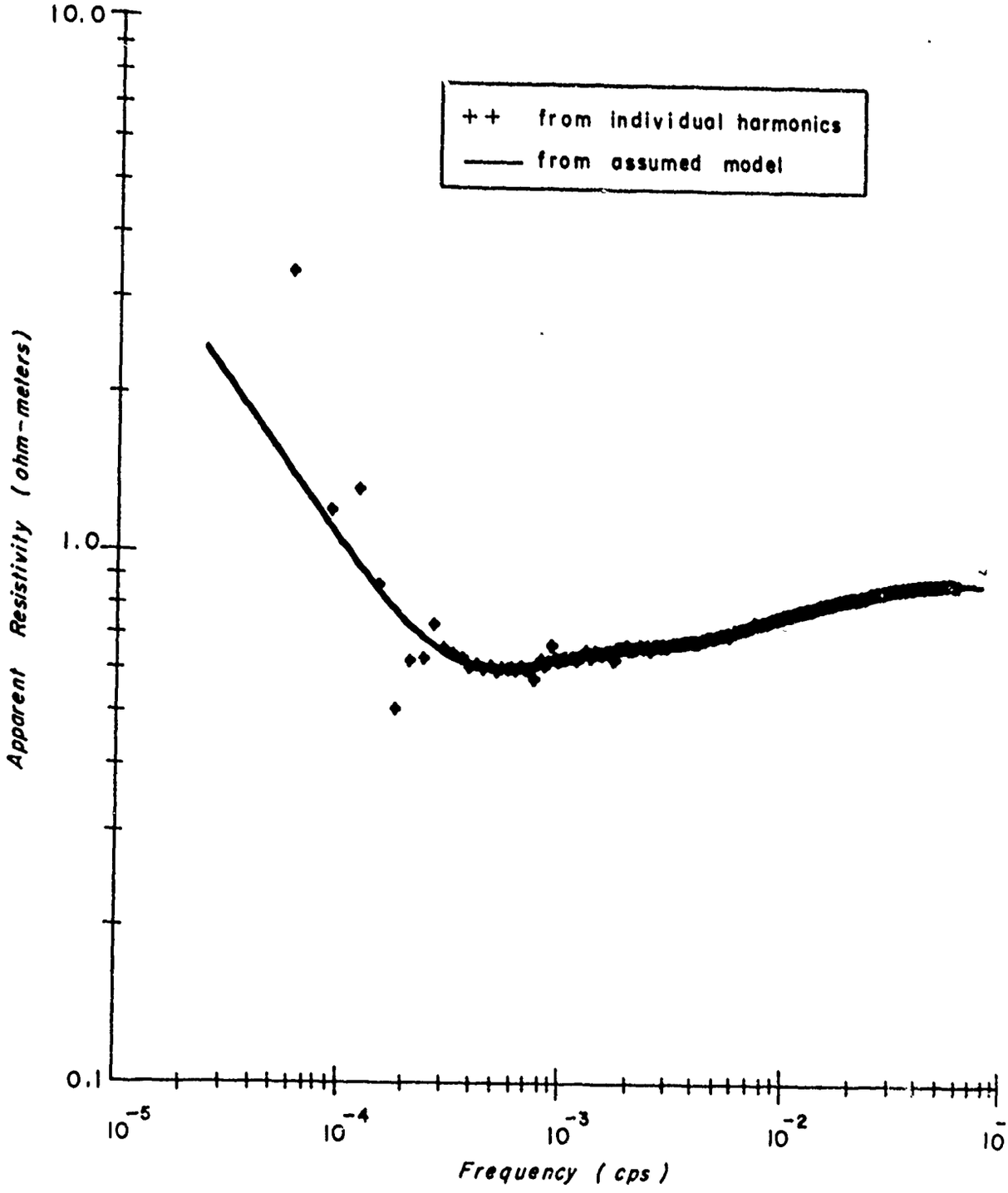

Fig. 18 Apparent Resistivity Estimates from Individual Harmonics of Truncated E and H Signals

BIBLIOGRAPHY

1. Blackman, R. B., Linear Data Smoothing and Prediction in Theory and Practice, Addison-Wesley, 1965.
2. Blackman, R. B., and J. W. Tukey, The Measurement of Power Spectra, Dover Publications, Inc., New York, 1959.
3. Bleil, D. F., Natural Electromagnetic Phenomena Below 30 kc/s, Plenum Press, New York, 1964.
4. Born, M., and E. Wolf, Principles of Optics, Pergamon Press, Inc., New York, 1965.
5. Bostick, F. X., Jr., and H. W. Smith, "An Analysis of the Magnetotelluric Method for Determining Subsurface Resistivities," Electrical Engineering Research Laboratory Report No. 120, The University of Texas at Austin, 1961.
6. Bostick, F. X., Jr., and H. W. Smith, "Investigation of Large-Scale Inhomogeneities in the Earth by the Magnetotelluric Method," Proceedings of the IRE, Vol. 50, No. 11, pp. 2339-2346, 1962.
7. Cagniard, L., "Basic Theory of the Magneto-Telluric Method of Geophysical Prospecting," Geophysics, Vol. 18, pp. 605-635, 1953.
8. Cantwell, T., "Detection and Analysis of Low Frequency Magnetotelluric Signals," Ph.D. thesis, Massachusetts Institute of Technology, 1960.
9. Cantwell, T., P. Nelson, J. Webb, and A.S. Orange, "Deep Resistivity Measurements in the Pacific Northwest," Journal of Geophysical Research, Vol. 70, No. 8, pp. 1931-1937, 1965.
10. Chapman, S., and J. Bartels, Geomagnetism, Oxford University Press, London, 1940.
11. Cooley, J. W., and J. W. Tukey, "An Algorithm for the Machine Calculation of Complex Fourier Series," Mathematics of Computation, Vol. 19, No. 90, pp. 297-301, 1965.

12. Eckhardt, D. H., "Theory and Interpretation of the Electromagnetic Impedance of the Earth," Journal of Geophysical Research, Vol. 73, No. 16, pp. 5317-5326, 1968.

13. d'Erceville, I., and G. Kunetz, "The Effect of a Fault on the Earth's Natural Electromagnetic Field," Geophysics, Vol. 27, No. 5, pp. 651-665, 1962.

14. Fournier, H. G., "Essai d'un Historique des Connaissances Magneto-Telluriques," Note 17, Institut de Physique du Globe, Universite de Paris, 1966.

15. Hancock, J. C., An Introduction to the Principles of Communication Theory, McGraw-Hill Book Company, Inc., New York, 1961.

16. Hopkins, G. H., jr., and H. W. Smith, "An Investigation of the Magneto-telluric Method for Determining Subsurface Resistivities," Electrical Engineering Research Laboratory Report No. 140, The University of Texas at Austin, 1966.

17. Kovtun, A. A., "The Magnetotelluric Investigation of Structures Inhomogeneous in Layers," Bulletin, Academy of Sciences, USSR, Geophys. Series, English Translation, pp. 1085-1087, 1961.

18. Madden, T. R., "Spectral, Cross-Spectral, and Bispectral Analysis of Low Frequency Electromagnetic Data," Natural Electromagnetic Phenomena Below 30 kc/s, Ed., D. F. Bleil, pp. 429-450, Plenum Press, New York, 1964.

19. Mann, J. E., "Magnetotelluric Theory of the Sinusoidal Interface," Journal of Geophysical Research, Vol. 69, No. 16, pp. 3517-3524, 1964.

20. Mann, J.E., "The Importance of Anisotropic Conductivity in Magneto-telluric Interpretation," Journal of Geophysical Research, Vol. 70, No. 12, pp. 2940-2942, 1965.

21. Morse, P. M., and H. Feshback, Methods of Theoretical Physics, McGraw-Hill Book Company, Inc., New York, 1953.

22. Neves, A. S., "The Magnetotelluric Method in Two Dimensional Structures," Ph.D. thesis, Massachusetts Institute of Technology, 1957.

23. Niblett, E. R., and C. Sayn-Wittgenstein, "Variation of Electrical Conductivity with Depth by the Magneto-Telluric Method," Geophysics, Vol. 25, pp. 998-1008, 1960.

24. Papoulis, A., Probability, Random Variables, and Stochastic Processes, McGraw-Hill Book Company, Inc., New York, 1965.

25. Patrick, F. W., "Magnetotelluric Modeling Techniques," Ph.D. thesis, The University of Texas at Austin, 1969.

26. Price, A. T., "The Theory of Magnetotelluric Methods when the Source Field is Considered," Journal of Geophysical Research, Vol. 67, No. 5, pp. 1907-1918, 1962.

27. Rankin, D., "A Theoretical and Experimental Study of Structure in the Magnetotelluric Field," Ph.D. thesis, University of Alberta, 1960.

28. Rankin, D., "The Magneto Telluric Effect on a Dike," Geophysics, Vol. 27, No. 5, pp. 666-676, 1962.

29. Rankin, D., G. D. Garland, and K. Vozoff, "An Analog Model for the Magnetotelluric Effect," Journal of Geophysical Research, Vol. 70, No. 8, pp. 1939-1945, 1965.

30. Rokityanski, I. I., "On the Application of the Magnetotelluric Method to Anisotropic and Inhomogeneous Masses," Bulletin, Academy of Sciences, USSR, Geophys. Series, English Translation, pp. 1050-1053, 1961.

31. Scholte, J. G., and J. Veldkamp, "Geomagnetic and Geoelectric Variations," Journal of Atmospheric and Terrestrial Physics, Vol. 6, No. 1, pp. 33-45, 1955.

32. Shanks, J. L., "Recursion Filters for Digital Processing," Geophysics, Vol. 32, No. 1, pp. 33-51, 1967.

33. Spitznogle, F. R., "Some Characteristics of Magnetotelluric Fields in the Soviet Arctic," Ph.D. thesis, The University of Texas at Austin, 1966.

34. Srivastava, S. P., "An Investigation of the Magnetotelluric Method for Determining Subsurface Resistivities," Ph.D. thesis, The University of British Columbia, 1962.

35. Srivastava, S. P., "Application of the Magnetotelluric Method to Anisotropic and Inhomogeneous Bodies," Journal of Geophysical Research, Vol. 68, No. 20, pp. 5857-5868, 1963.

36. Swift, C. M., Jr., "A Magnetotelluric Investigation of an Electrical Conductivity Anomaly in the Southwestern United States," Ph.D. thesis, Massachusetts Institute of Technology, 1967.

37. Tikhonov, A. N., N. V. Lipskaya, and B. M. Yanovsky, "Some Results of the Deep Magneto-Telluric Investigations in the USSR," Journal of Geomagnetism and Geoelectricity, Vol. 15, No. 4, pp. 275-279, 1964.

38. Vozoff, K., H. Hasegawa, and R. M. Ellis, "Results and Limitations of Magnetotelluric Surveys in Simple Geologic Situations," Geophysics, Vol. 28, No. 5, pp. 778-792, 1963.

39. Wait, J. R., "On the Relation Between Telluric Currents and the Earth's Magnetic Field," Geophysics, Vol. 19, pp. 281-289, 1954.

40. Wait, J. R., Electromagnetic Waves in Stratified Media, MacMillan Company, New York, 1962.

41. Word, D. R., "An Investigation of the Magnetotelluric Tensor Impedance Method," Ph.D. thesis, The University of Texas at Austin, 1969.

UNCLASSIFIED
Security Classification

DOCUMENT CONTROL DATA - R & D

(Security classification of title, body of abstract and indexing annotation must be entered when the overall report is classified)

1. ORIGINATING ACTIVITY (Corporate author)	2a. REPORT SECURITY CLASSIFICATION
The University of Texas at Austin Electronics Research Center Austin, Texas 78712	UNCLASSIFIED 2b. GROUP

3. REPORT TITLE

METHODS OF MAGNETOTELLURIC ANALYSIS

4. DESCRIPTIVE NOTES (Type of report and inclusive dates)

Scientific Interim

5. AUTHOR(S) (First name, middle initial, last name)

William E. Sims F. X. Bostick, Jr.

6. REPORT DATE	7a. TOTAL NO. OF PAGES	7b. NO. OF REFS
7 January 1969	94	41

8a. CONTRACT OR GRANT NO.	9a. ORIGINATOR'S REPORT NUMBER(S)
AF-AFOSR-67-766E b. PROJECT NO. 4751 c. 6144501F d. 681305	JSEP, Technical Report No. 58 9b. OTHER REPORT NO(S) (Any other numbers that may be assigned this report) AFOSR 69-0189 TR

10. DISTRIBUTION STATEMENT

1. This document has been approved for public release and sale; its distribution is unlimited.

11. SUPPLEMENTARY NOTES	12. SPONSORING MILITARY ACTIVITY
TECH, OTHER Research sponsored by NSF Grant GA-1236 and ONR Contract N00014-A-0126-0004	JSEP through AF Office of Scientific Research (SREE) 1400 Wilson Boulevard Arlington, Virginia 22209

13. ABSTRACT

Magnetotelluric prospecting is a method of geophysical exploration that makes use of the fluctuations in the natural electric and magnetic fields that surround the earth. These fields can be measured at the surface of the earth and they are related to each other by a surface impedance that is a function of the conductivity structure of the earth's substrata.

This report describes some new methods for analyzing and interpreting magnetotelluric data. A discussion is given of the forms of the surface impedance for various classes of models, including one, two and three dimensional models. Here, an n dimensional model is one in which the parameters describing the model are functions of at most n space coordinates. Methods are discussed for estimating the strike direction for data that is at least approximately two dimensional. A new linearized approach to the one dimensional problem is discussed. Subject to the approximations of the linearization, it is shown that under appropriate transformations of the frequency and depth scales, the reciprocal of the surface impedance as a function of frequency is equal to the square root of the conductivity as a function of depth convolved with a linear response function that is somewhat like a low pass filter.

Included in this report is a comparison of several methods of estimating the auto and cross power density spectra of measured field data, and of several methods for estimating the surface impedance from these spectra. The effects of noise upon these estimates are considered in some detail. Special emphasis is given to several types of artificial noise including aliasing, round off or digitizer noise, and truncation effects. Truncation effects are of the most interest since they depend upon the particular window used in the spectral analysis.

DD FORM 1 NOV 65 1473

UNCLASSIFIED
Security Classification

14. KEY WORDS	LINK A		LINK B		LINK C	
	ROLE	WT	ROLE	WT	ROLE	WT
MAGNETOTELLURICS						
DATA ANALYSIS						